In Silico Assessment of 5-FU Therapy via A Mathematical Model with Fuzzy Uncertain Parameters

Sajad Shafiekhani
Tehran University of Medical Sciences
Amir. H. Jafari
Tehran University of Medical Sciences
L. Jafarzadeh
Tehran University of Medical Sciences
N. Gheibi (gheibi_n@yahoo.com)

Research

Keywords: ODE, Fuzzy, Uncertain, 5-FU

Posted Date: July 6th, 2020

DOI: https://doi.org/10.21203/rs.3.rs-39994/v1

Title: In Silico Assessment of 5-FU Therapy via a Mathematical Model with Fuzzy Uncertain Parameters

S. Shafiekhani[1, 2, 3, 4], A. H. Jafari[1, 2], L. Jafarzadeh[5], N. Gheibi[4*]

[1]Departments of Biomedical Engineering, School of Medicine, Tehran University of Medical Sciences.

[2]Research Center for Biomedical Technologies and Robotics, Tehran, Iran.

[3]Students' Scientific Research Center, Tehran University of Medical Sciences, Tehran, Iran.

[4]Cellular and molecular research center, Qazvin University of Medical Science, Qazvin, Iran.

[5]Department of Medical Immunology, School of Medicine, Tehran University of Medical Sciences, Tehran, Iran.

Abstract:

Background: Ordinary differential equation (ODE) models widely have been used in mathematical oncology to capture dynamics of tumor and immune cells and evaluate the efficacy of treatments. However, for dynamic models of tumor-immune system (TIS), some parameters are uncertain due to inaccurate, missing or incomplete data, which has hindered the application of ODEs that require accurate parameters.

Methods: We extended an available ODE model of TIS interactions via fuzzy logic to illustrate the fuzzification procedure of an ODE model. Fuzzy ODE (FODE) models, in comparison with the stochastic differential equation (SDE) models, assigns a fuzzy number instead of a random number (from a specific probability density function) to the parameters, to capture parametric uncertainty. We used FODE model to predict tumor and immune cells dynamics and assess the efficacy of 5-FU. The present model is configurable for 5-FU chemotherapy injection timing and propose testable hypothesis in vitro/ in vivo experiments.

Result: FODE model was used to explore the uncertainty of cells dynamics resulting from parametric uncertainty in presence and absence of 5-FU therapy. In silico experiments revealed that the frequent 5-FU injection created a beneficial tumor microenvironment that exerted detrimental effects on tumor cells by enhancing the infiltration of CD8+ T cells, and NK cells, and decreasing that of myeloid-derived suppressor (MDSC) cells. We investigate the effect of perturbation on model parameters on dynamics of cells through global sensitivity analysis (GSA) and compute correlation between model parameters and cell dynamics.

Conclusion: ODE models with fuzzy uncertain kinetic parameters cope with insufficient experimental data in the field of mathematical oncology and can predict cells dynamics uncertainty band. In silico assessment of treatments considering parameter uncertainty and investigating the effect of the drugs on movement of cells dynamics uncertainty band may be more appropriate than in crisp setting.

Keywords: ODE, Fuzzy, Uncertain, 5-FU

Introduction:

Cancer related death is regarded as one of the leading causes of death around the world. According to global statistics, 27.5 million people will be diagnosed with cancer by 2040[1]. The immune system can organize immune responses and eliminate tumor cells by identifying tumor antigens. However, tumor cells have evolved into different pathways to escape immune surveillance and metastasize to other tissues. The immune system consists of two general types: innate immunity and adaptive immunity[2][3].

Natural killer cells (NK cells) are cells of the innate immunity which act as first line of defense against cancer cells. Natural killer cells prevent tumor growth with various mechanisms such as direct cell destruction, induction of programmed death (through the expression of death-inducing Ligand (Fas), and tumor necrotic factor (TNF)-related apoptosis-inducing ligand (TRAIL)), production of proinflammatory factors such as Interferon-gamma (IFN- γ) and Nitrite oxide (NO)[4] . Regarding adaptive immunity, Cytotoxic T cells (CTL) are the most competent cells against tumor cells. Regulatory T cells (Treg) and Myeloid-Derived Suppressor Cells (MDSC) are also recruited to the tumor microenvironment for modulating the immune responses in the tumor site[5][6]. MDSCs abundant in tumor tissues and secondary lymph nodes. MDSCs have inhibitory effects on the immune response to tumor cells through production of inhibitory cytokines such as interleukin 10 (IL-10), transforming growth factor β (TGF-β), by production of reactive oxygen species (ROS), NO, Indoleamine oxidase (IDO), induction of Treg cells and inhibitory effect on anti-tumor function of NK cells[7][8][9]. Chemotherapy drugs such as Gemcitabine, 5-Fluorouracil (5-FU), and paclitaxel suppress the activity and production of MDSCs, enhancing the protective immune responses against tumors[10][11][12]. Although many studies have pointed to the positive effects of inhibiting MDSCs for tumor treatment, the efficacy of the 5-FU treatment has remained questionable and requires further investigation[13][14][15]. In addition, due to the complex dynamic responses elicited by the immune system against tumor cells[16][17], and also inherent noise and fluctuations in signaling pathways and regulatory networks that control different functions of cells, and uncertainty in the kinetic/dynamic rate of tumor-immune system interactions[18], there is a demanding need for new class of computational models to predict dynamics of TIS agents in uncertain environment.

In general, computational models for tumor-immune system interactions can be categorized into two groups including deterministic models and stochastic models[19][20]. Taking into account all the interactions of the system in the form of pre-defined relationships with exact equations, deterministic models can simulate the dynamics of the model components without regarding uncertainty in behaviors of cells and in their interactions. The ordinary differential equation (ODE) models as deterministic models, widely have been used in systems biology[21][22][23][24][25]. Due to the lack of comprehensive knowledge about how biological processes (from subcellular networks to cell-cell interactions) occurs, there is a structural uncertainty. Also, because of dynamic features of biological networks during time and from patient to patient, error in data acquisition, incomplete or missing data, etc., estimating the exact (crisp value) rate of different behaviors of cells (for example, the rate of apoptosis, expansion, recruitment, etc.) is inconceivable[26][27][28]. Therefore, deterministic models that can simulate this amount of biological detail will have very complex relationships and many parameters that are constrained by the lack of enough precise experimental data. On the other hand, stochastic models with assigning specific probability density functions (pdf) for different behaviors of cells and by probabilistic rules for simulating cell-cell interactions can simulate the behavioral uncertainty

and inherent noise in tumor-immune system[29][30][31][32]. Often, stochastic models versus deterministic models require fewer kinetic parameters to predict dynamics, but they are computationally cost. It seems that, by assigning fuzzy uncertain numbers instead of crisp values in kinetic/dynamic rate of cells in deterministic models, and without using stochastic rules or assigning specific pdf for the rate of different behaviors of cells, we can capture dynamics of tumor-immune system in uncertain environment. Therefore, we can use deterministic models with fuzzy uncertain kinetic parameters instead of stochastic models that often are computationally cost. In order to investigate the efficacy of 5-FU treatment in suppressing MDSCs and tumor cells in the inflammatory environment and dynamically analyzing the tumor-immune system interactions, a mathematical model with fuzzy uncertain parameters for the NK cells, MDSCs and CTLs interactions with tumor cells has been developed. By considering some of the kinetic parameters of the model as being fuzzy, current mathematical model studied the effect of uncertainty on kinetic parameters on the dynamics of cancer and immune cells and also analyzed the effect of 5-FU therapy in uncertain environment.

Fuzzy theorem describes 'possibility', different from ‘probability’ theorem which studies random processes[33]. Fuzzy sets have the capability to deal with uncertain information. Fuzzy sets describe uncertainty caused by ambiguity, lack of knowledge, incomplete or missing data, imprecision and errors of measurements. Since fuzzy uncertainty is an inherent feature of biological networks, many models in the systems biology are based on fuzzy knowledge[34][35][36]. In a study, a fuzzy inference system (FIS) was used to calculate the interaction rates of the continuous Petri net model[37]. It was shown that this model with the lowest kinetic parameters (often unavailable due to lack of experimental data) and using linguistic rules (qualitative description) about the interacting cells was able to capture the dynamics of the TIS agents and simulate its behaviors[37]. In two recent studies, fuzzy parameters were used to model the uncertainties in the kinetic parameters of stochastic Petri net [38]and continuous Petri net[39]. Current study aimed to use fuzzy uncertain kinetic parameters for the ODE model and create a FODE model. This model was used to simulate TIS behaviors assigning fuzzy and crisp values for kinetic parameters and evaluate the efficacy of 5-FU treatment in both crisp and fuzzy setting.

Mathematical modeling widely has been used to investigate the efficacy of different treatment strategies for various cancers. For instance, in a recent study the efficacy of L-arginine and 5-FU therapies for the treatment of lymphoma (El4-luc2 cell line), breast cancer (4T1 cell line) and lung carcinoma (3LL cell line) by a system of ODEs was evaluated[40]. For the same purpose, in another study, combination of radiotherapy and anti-PD-1 therapy by a discreet-time mathematical model was evaluated and temporal dynamics of TIS agents were captured[41]. Also in an another study, the combination of vaccine (GVAX) and anti-PD-1 therapy by a set of partial differential equations was evaluated and spatio-temporal dynamics of TIS constituents *in silico* environment was assessed[42]. Also, in another study, the effect of anti-PD-1/PD-L1 therapy and anti-CTLA-4 using a set of ODEs and pharmacokinetic pharmacodynamics equations was investigated[43]. All of these studies explored the efficacy of different treatment strategies regarding crisp values for kinetic parameters, whereas in biological networks including TIS, various sources of uncertainty exist that should be considered in the computational model[44][45]. Current study aimed to evaluate the efficacy of 5-FU treatment in fuzzy uncertain environment (in different setting of fuzzy parameters) and explore how uncertainty in kinetic parameters of model affects the dynamics of TIS agents in different modalities of 5-FU

treatment. For this purpose, present study developed a fuzzy ordinary differential equation (FODE) model to capture uncertain dynamical behavior of TIS agents and investigate how different regimens of 5-FU therapy causes the uncertainty band of tumor cells and immune cells to move.

Methods:

The first part of methods describes the tumor-immune system and explain the detail of ODE formulation of system. In the next section, we describe how fuzzify the kinetic parameters of an ODE to capture uncertainty band of model's constituents in response to fuzzy uncertainty of kinetic parameters. After that, the results of this study are presented.

Structure of ODE model of TIS:

The mathematical model of tumor-immune system interactions of this study was adapted from the model developed by *shariatpanhi et al*[40]. The structure of model is based on ordinary differential equation that with deterministic rates simulates the biological and biophysical/biochemical behaviors of TIS agents. TIS of this study consist of tumor cells, NK cells, CTLs and MDSCs. Equation (1) describes the dynamics of tumor cells, which consists of four terms. The term $aClog\left(\frac{Cmax}{C}\right)$ describes tumor cell growth rate in absence of treatment with carrying capacity$Cmax$, the term bNC^* and term ηTC^* describes NK-mediated tumor cell killing rate and CTL-mediated tumor killing rate, respectively. The term dC describes therapeutic effect of 5-FU, which reduces the tumor cell population by up to 3 days after treatment ($d = 0.7$), and then the effect of the 5-FU disappears ($d = 0$). Equation (2) describes dynamics of NK cells, which consist of four terms. The term σ describes constant influx rate of NK cells in tumor microenvironment, fN explains exponential apoptosis rate of NK cells, $g\frac{NC^2}{\mathrm{h}+C^2}$ and pNC^* describe the recruitment rate of NK cells into the tumor microenvironment and inactivation rate of encountered NK cells with tumor cells, respectively. Equation (3) models dynamics of CTLs, which consist of five terms. mT describes exponential apoptosis rate of CTLs, $j\frac{TC^2}{k+C^2}$ describes the recruitment rate of CTLs into the tumor microenvironment, rNC^*S explains the activation rate of CTLs as a result of interactions of NK cells and accessible tumor cells that this stimulation rate is inhibited by MDSCs. The uTC^* and vT describe the inactivation rate of CTLs after encountering with accessible tumor cells and differentiation rate of CTLs into other phenotypes of T cells such as regulatory T cells (Tregs), respectively. Equation (4) describes the suppressive effect of MDSCs on stimulation rate of CTLs. Equation (5) explains the dynamics of MDSCs, ρ explains production rate of splenic MDSCs, βM and $\alpha\frac{C}{q+C}$ describe the MDSCs' exponential apoptosis rate and their expansion rate in inflammatory environment, respectively. The full description of kinetic parameters of equations (1) to equation (5) is given in table 1.

$$\frac{dC}{dt} = aClog\left(\frac{Cmax}{C}\right) - bNC^* - \eta TC^* - dC\,,\ C^* = \frac{C}{(1+\frac{C^{1/3}}{l})} \tag{1}$$

$$\frac{dN}{dt} = \sigma - fN + g\frac{NC^2}{\mathrm{h}+C^2} - pNC^* \tag{2}$$

$$\frac{dT}{dt} = -mT + j\frac{TC^2}{k + C^2} + rNC^*S - uTC^* - vT \quad (3)$$

$$S = \frac{1 - Smin}{1 + \gamma(M - Mmin)^2} + Smin \quad (4)$$

$$\frac{dM}{dt} = \rho - \beta M + \alpha\frac{C}{q + C} \quad (5)$$

Fuzzy Ordinary Differential Equation (FODE)

A fuzzy set A of universal set χ is defined by its membership function:

$$\mu_A: \chi \rightarrow [0, 1] \quad (6)$$

which for an element $x \in \chi$, determines the value $\mu_A(x)$ as the membership degree of element x in fuzzy set A. The value $\mu_A(x) = 0$ means that the element x is not a member of a fuzzy set A and the value $\mu_A(x) = 1$ means that the element x fully belongs to the fuzzy set A. The values $0 < \mu_A(x) < 1$ characterize fuzzy members, which partially belong to the fuzzy set A.

In first step, the fuzzy number A of uncertain kinetic parameter is partitioned into α-cuts, $\alpha \in [0, 1]$ with k levels, which the ith level of α is $\alpha_i = \frac{k-i}{k-1}, i\epsilon\{1,2,\ldots,k\}$. Also, α_i of fuzzy set $\boldsymbol{A}$ is a crisp subset of $\boldsymbol{X}$, i.e., $\boldsymbol{A}_{\alpha_i}=\{\boldsymbol{x}|\ \mu_{\boldsymbol{A}}(\boldsymbol{x}) \geq \alpha_i, \mathbf{x} \in \boldsymbol{X}, \alpha_i \in [0, 1]\}$. Then discretize the values $\boldsymbol{x}$ of crisp subset $\boldsymbol{A}_{\alpha_i}$ of the ith α-cuts (α_i) to J points, therefore we create a subset $\boldsymbol{\phi_x} = \{x_1, x_2, \ldots, x_J\}$ (in this study number of the discretization points for each α-cut is J=5) and execute the ODE model with parameters $x_j \in \boldsymbol{\phi_x}. j = \{1,2,,,J\}$ and find minimum and maximum of population/concentration of each of cells/cytokines (outcome measure) to capture minimum and maximum band of uncertainty of outcome measures in this α-cut. By increasing the α value, the uncertainty band in the input parameter of the model decreases and if, α=1, there is no uncertainty for kinetic parameter (similar to ODE model with crisp kinetic parameter). Therefore, with this simple method, we can apply uncertainty to model kinetic parameters and compute the dynamic of cells to find uncertainty bands of cells/cytokines dynamics.

In the following, we describe the algorithm of fuzzification of kinetic parameters of ODE model.

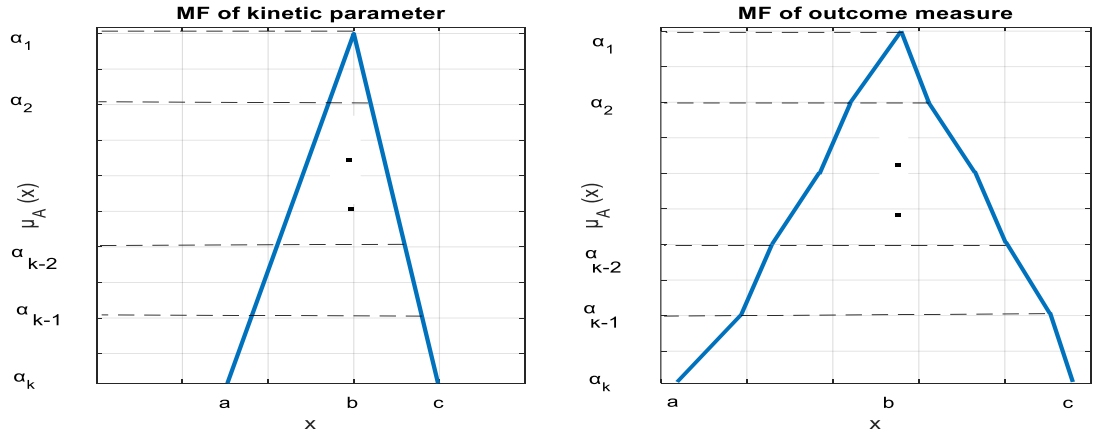

Figure 1. (Left) Decomposition of a fuzzy uncertain kinetic parameter to its α-cuts and (right) composition of a set of α-cuts to create a membership function for fuzzy uncertain outcome measure.

Input: A FODE model.

Output: an uncertain band of each outcome measure.

1: **For each** α level, $\alpha_i, i = 1,2, \dots, k$ **do**

2: **For each** fuzzy number from uncertain kinetic parameters, denoted by $\ddot{O}_l, l = 1,2, \dots, L$ **do**

3: Compute α-cuts of fuzzy parameter, represented as $\boldsymbol{A}_{\alpha_i} = \left[L_l^i, U_l^i\right]$;

4: Discretize each α-cut, $\boldsymbol{A}_{\alpha_i}$ and obtain J crisp values for each fuzzy uncertain number.

5: **end for**

6: **For each** combination $c \in J^L$ of crisp values for all fuzzy uncertain parameters **do**

7: Run ODE model for each combination to obtain dynamics $Y_c^i\left(c \in J^L\right)$

8: Obtain the minimum ($MinUncertaintyOutput^i = \min_{c \in J^L}(Y_c^i)$) and maximum ($MaxUncertaintyOutput^i = \max_{c \in J^L}(Y_c^i)$) .

9: **end for**

10: Compute the uncertainty band (membership function) for each outcome measure

11: **For each** record of dynamics of model **do**

12: $UpperBand = max_{i=1,2,\dots,I}\left(MaxUncertaintyOutput^i\right)$

13: $LowerBand = min_{i=1,2,\dots,I}\left(MinUncertaintyOutput^i\right)$

14: **end for**

In the following, crisp and fuzzy parameters of TIS's model are set using values from table 1 and table 2, respectively. All simulations in both crisp and fuzzy settings were run in MATLAB 2019a.

Table 1. Crisp values of TIS parameter.

Parameter	Unit	Value	Biological Description	refer ence	Parameter	Unit	value	Biological Description	Reference
a	$\frac{1}{day}$	1.45×10^{-1}	El4-luc2 tumor growth rate in absence of treatment	[40]	m	$\frac{1}{day}$	2×10^{-2}	Exponential death rate of CTLs	[40]
$Cmax$	$cell$	1×10^{10}	Tumor carrying capacity	[40]	j	$\frac{1}{day}$	1×10^{-1}	Maximum recruitment rate of CTLs	[40]
b	$\frac{1}{cell \times d}$	3.23×10^{-7}	NK-mediated tumor killing rate	[40]	k	$cell^2$	2.02×10^{7}	Steepness coefficient of the CTL recruitment curve	[40]
η	$\frac{1}{cell \times d}$	1.1×10^{-7}	CTL-mediated tumor killing rate	[40]	r	$\frac{1}{cell \times}$	1.1×10^{-7}	Stimulation rate of CTLs as a result of tumor and NK cell interactions	[40]
d	$\frac{1}{day}$	0.7	EL4-luc2 tumor apoptosis rate by low dose 5-FU treatment	[40]	u	$\frac{1}{cell \times}$	1×10^{-10}	Inactivation rate of CTLs after encounter with the tumor	[40]
l	$cell^{\frac{1}{3}}$	100	Depth of access of immune cells to tumor cells	[40]	v	$\frac{1}{day}$	1×10^{-2}	Differentiation rate of CTL cells to other T cells	[46]
σ	$\frac{cell}{day}$	1.4×10^{4}	Constant influx rate of NK cells	[40]	$Smin$	$none$	0.18	Minimum CTL proliferation factor due to inhibition by MDSCs	[40]
f	$\frac{1}{day}$	4.12×10^{-2}	Exponential death rate of NK cells	[40]	γ	$cell^{-2}$	6×10^{-3}	Inhibition rate of CTL stimulation by MDSCs	[40]
g	$\frac{1}{day}$	2.5×10^{-2}	Maximum recruitment rate of NK cells	[40]	$Mmin$	$cell$	2.5×10^{6}	Normal number of MDSCs in C57/BL6 mice	[40]
h	$cell^2$	2.02×10^{7}	Steepness coefficient of the NK cell recruitment curve	[40]	ρ	$\frac{cell}{day}$	$0.25 \times Mmin$	Normal production rate of MDSCs	[40]
p	$\frac{1}{cell \times d}$	1×10^{-7}	Inactivation rate of NK cells after encounter with the tumor	[40]	β	$\frac{1}{day}$	0.25	Exponential death rate of MDSCs	[40]
q	$cell$	1×10^{10}	Steepness coefficient of the MDSCs production curve	[40]	α	$\frac{cell}{day}$	7×10^{6}	MDSC expansion rate in EL4-luc2 tumor-bearing mice	[40]

Table 2. Fuzzy values of TIS parameters.

Parameter	Triangular fuzzy membership function parameters
a	$(\mathbf{0.9}, \mathbf{1}, \mathbf{1.1}) \times \mathbf{1.45 \times 10^{-1}}$

f	$(\mathbf{0.9, 1, 1.1}) \times \mathbf{4.12 \times 10^{-2}}$
m	$(\mathbf{0.9, 1, 1.1}) \times \mathbf{2 \times 10^{-2}}$
α	$(\mathbf{09, 1, 1.1}) \times \mathbf{7 \times 10^{6}}$

Results:

We begin with evaluation of model in crisp setting (Table 1) in which no uncertainty exists in kinetic parameters. We simulate the TIS interactions to predict dynamics of cells and evaluate the efficacy of different regimens (timing) of 5-FU treatment by in-silico experiments. It has shown that slow accumulation of immune suppressive cells such as MDSCs, Treg and other immune-suppressive cells mediates tumor cell re-growth, 18 to 20 days after tumor injection. Therefore, we start 5-FU treatment from day 10 after tumor inoculation to inhibit the immune-suppressive effect of MDSCs in inflammatory environment[47].

Figure 2.A (Figure 2.B) shows the dynamics of tumor cells, NK cells, CTLs and MDSCs in crisp setting and by applying 5-FU chemotherapy on days 10:6:22 after tumor inoculation on day 0 (under 5-FU treatment on days 10:6:76). Figure 2.C and Figure 2.D show the inhibition percentage of instantaneous tumor cell population by applying 5-FU treatment on days 10:6:22 and on days 10:6:76, respectively. Assessment of model for different 5-FU chemotherapy injection timings revealed that by 3 injections of 5-FU (induction on days 10:6:22 after tumor inoculation on day 0), the tumor volume on day 100 was 600 times that of its initial value, whereas with ten 5-FU injections (in days 10:6:76 after tumor inoculation on day 0), 100 days after tumor induction, the tumor volume was reduced to 1% of its initial inoculated value. Therefore, the simulations revealed that with increasing 5-FU injections, the tumor no longer grows and is almost eliminated while with less 5-FU injections, it is possible that the controlled tumor regrowth and metastasize. To investigate the efficacy of 5-FU treatment for inhibiting the instantaneous tumor cell population, we compute the inhibition percentage of tumor cells affected by different timings of 5-FU treatment (10:6:22 in Figure 2.C and 10:6:76 in Figure 2.D). As it's depicted in Figure 2.C, 3-time injection of 5-FU causes the tumor inhibition percentage on days 25 reaches its maximum level (because the last injection was on day 22 and the effect of 5-FU remains until three days after induction), and after that, the effect of drug disappeared and tumor regrowth. By increasing 5-FU injections (10:6:76), as depicted in Figure2.D, the instantaneous tumor inhibition percentage remains close to 98% (even after discontinuation of 5-FU treatment on day 76) and the tumor cells are eliminated.

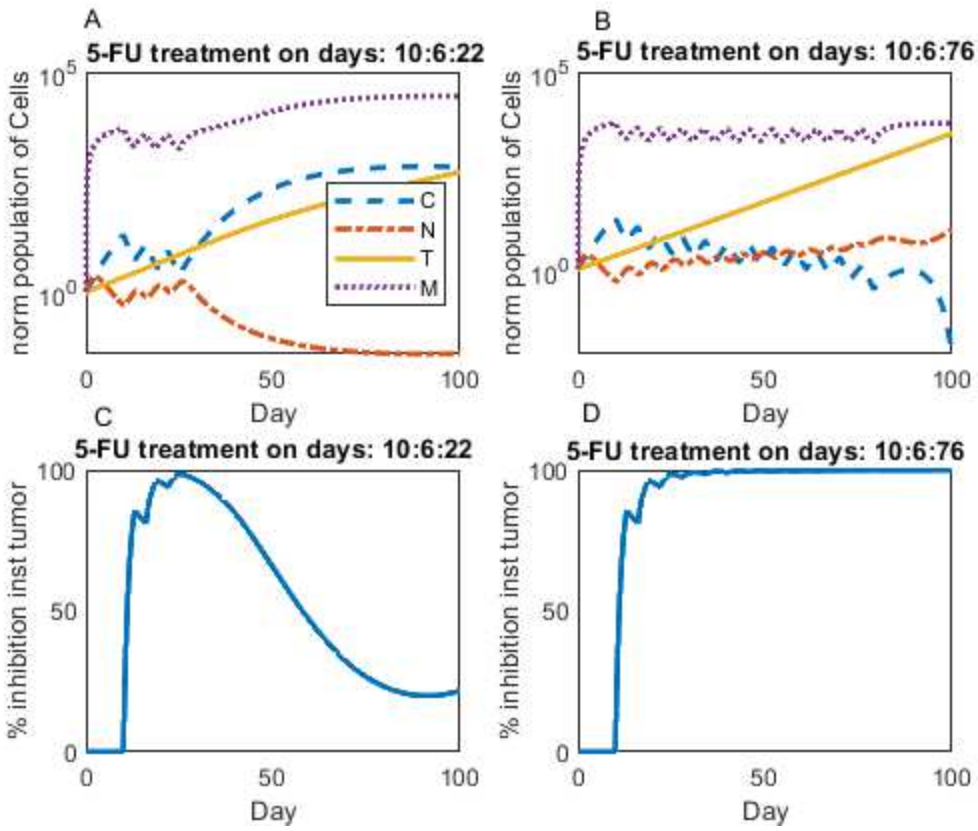

Figure 2. Dynamics of tumor cells, NK, CTL, and MDSC in response to different timing of 5-FU treatment over time along with efficacy assessment of 5-FU treatment with regarding crisp values for kinetic parameters of model. (A) The dynamics of cancer cells, NK cells, CTLs and MDSCs (normalized to initial population) affected by 5-FU treatment on days 10, 16 and 22 after tumor injection on day 0 and (B) by 5-FU treatment on days 10, 16, 22, 28, 34, 40, 46, 52, 58, 64, 70 and 76 after tumor injection on day 0. (C) The instantaneous inhibition percentage of tumor cells affected by 5-FU on days 10:6:22 and (D) by 5-FU treatment on days 10:6:76.

We found that frequent 5-FU treatment would inhibit the tumor, so for further investigation, we increased the frequency of 5-FU treatment from three times (days 10:6:22) to twelve times (days 10:6:76) to capture the dynamics of inhibition percentage of tumor cells (Figure 3.A) and MDSCs (Figure 3.B) and the dynamics of relative population of NK cells (Figure 3.C) and CTLs (Figure 3.D) in treatment case to no treatment case. As the frequency of 5-FU treatment increases, the percentage of tumor cell suppression, percentage of MDSC suppression and population of NK cells and CTLs increase, respectively. This subject that antitumor treatment can improve the tumor microenvironment to exert detrimental effects on tumor cells, has been investigated in previous experimental studies. For example in a B16-F10 melanoma-bearing mice model, it was shown that the combination of radiotherapy and hyperthermia enhanced the infiltration of CD8+ T cells, NK cells and CD11c + /MHCII + /CD86+ dendritic cells, and decreased that of myeloid-derived suppressor cells and regulatory T cells[48]. In another study, the authors found that 5-FU at low doses can boost circulating NK cells[49]. Also, 5-FU has been used in acute pancreatitis to minimize the abnormal immune cytokines[50]. In this study, in silico experiments revealed that 5-FU can enhance the infiltration of NK cells

(as depicted in Figure 3.C) and CTLs (Figure 3.D) in tumor microenvironment and subsequently suppress MDSCs (Figure 3.B) and tumor cells (Figure 3.A).

We simulate the TIS in fuzzy uncertain setting to capture uncertainty band of tumor cells, NK cells, CTLs and MDSCs in presence or absence of 5-FU treatment. To investigate the effect of uncertainty of kinetic parameters on dynamics of cells and for efficacy assessment of different timings of 5-FU treatment in fuzzy uncertain environment, we simulate TIS by setting the values of parameters (a, f) and (a, f, m, α) to fuzzy numbers, and three times (10:6:22) and twelve times (10:6:76) of 5-FU injection. Figure 4. A, Figure 4. B, Figure 4. C and Figure 4. D shows the uncertainty region of cancer cells, NK cells, CTLs and MDSCs, respectively, with regarding two uncertain kinetic parameters (a, f). The membership function of uncertain parameters a and f are triangular (as described in Table 2). We assign three α levels for fuzzy numbers ($\alpha = 0$, $\alpha = 0.5$ and $\alpha = 1$), that with the increase of α from 0 to 1, the uncertainty band of kinetic parameter decreases. Actually, $\alpha = 0$ corresponds to maximum uncertainty for parameters and $\alpha = 1$ corresponds to crisp setting of model (no uncertainty exists). We show that with increasing the frequency of 5-FU treatment from three times to teve12 times, the population of cancer cells and MDSCs decrease (their uncertainty band shift left toward lower population of cells) and the population of NK cells and CTLs increase (their uncertainty band shift right toward higher population of cells). Also, with increasing the uncertainty level α from 1 to 0, the uncertainty band of all cells increases. Therefore, 5-FU efficacy was demonstrated in both crisp and fuzzy settings. Figure 5 depicts the results of model simulation with four fuzzy uncertain numbers as mentioned in Table 2. To explore the effect of different timings of 5-FU injection (10:6:22, 10:6:34, 10:6:46, 10:6:58, 10:6:76) on uncertainty band of tumor and immune cells, we simulated TIS with two and four uncertain parameters. As depicted in Figure 6 (two uncertain parameters) and Figure 7(four uncertain parameters), by increasing the times of 5-FU injection shift the uncertainty band of tumor cells and MDSCs to left and shift the uncertainty band of NK cells and MDSCs to right.

In next analysis, we want to explore the effect of increasing the number of fuzzy uncertain parameters (from two parameters to four). We expect the cell uncertainty band to increase as the number of fuzzy parameters increases. This result is illustrated in Figures 8.C (membership function of CTLs with regarding 5-FU injection on days 10:16:22), 6.D (membership function of MDSCs with regarding 5-FU injection on days 10:16:22), 9.C (membership function of CTLs with regarding 5-FU injection on days 10:16:76) and 9.D (membership function of MDSCs with regarding 5-FU injection on days 10:16:22). With the increase of fuzzy uncertain numbers from two to four, the uncertainty band of cancer cells and NK cells do not change (due to insensitivity of cancer cells and NK cells to parameters m, α), while the uncertainty band of CTLs and MDSCs expand.

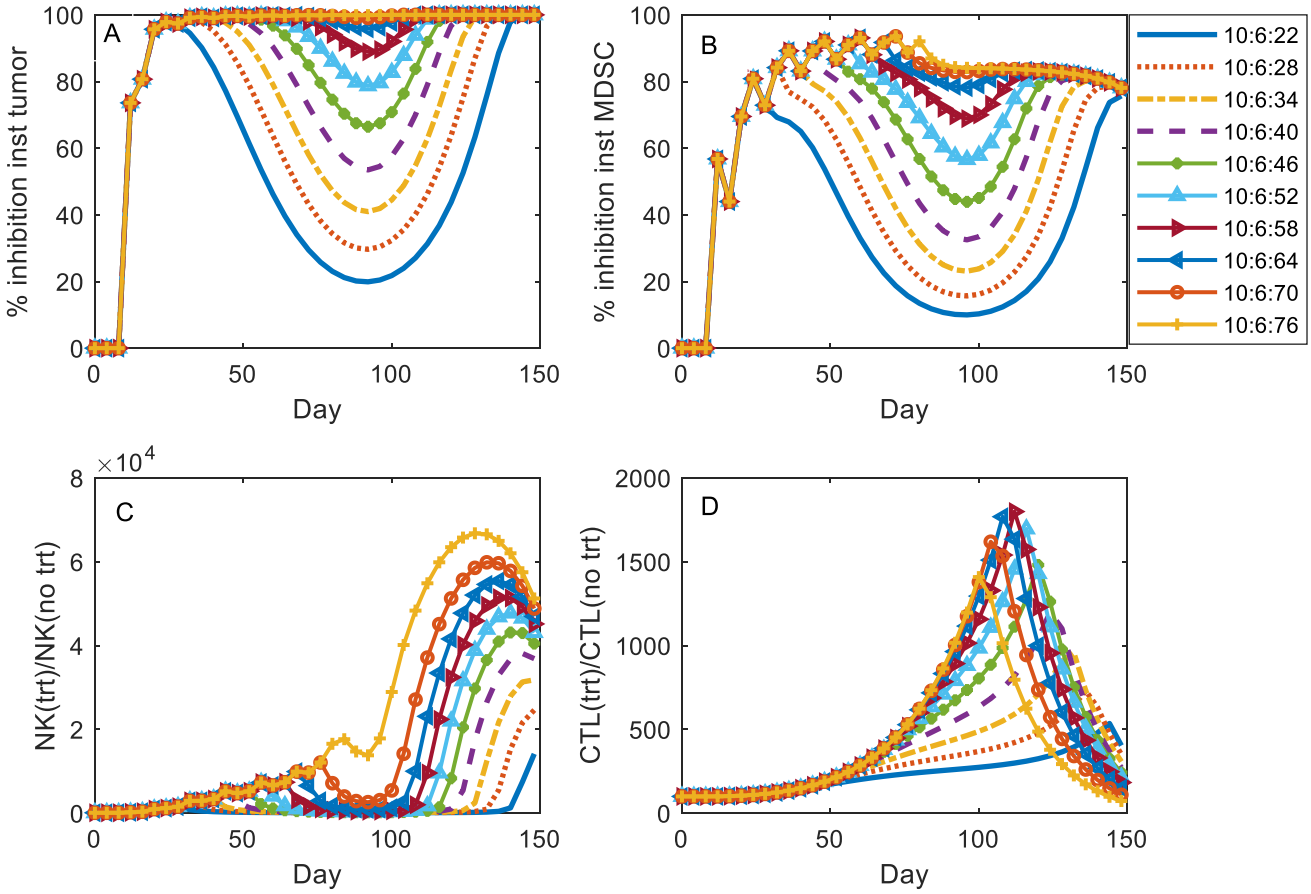

Figure 3. Prediction of the effect of different timing of 5-FU treatment on TISTIS cells population. The treatment efficacy for different timing of 5-FU was plotted as percentage of instantaneous tumor growth inhibition (A) and percentage of instantaneous MDSC expansion inhibition (B). The ratio of population of NK cells (C) and CTLs (D) in different timing of 5-FU treatment to their population in control case (no treatment).

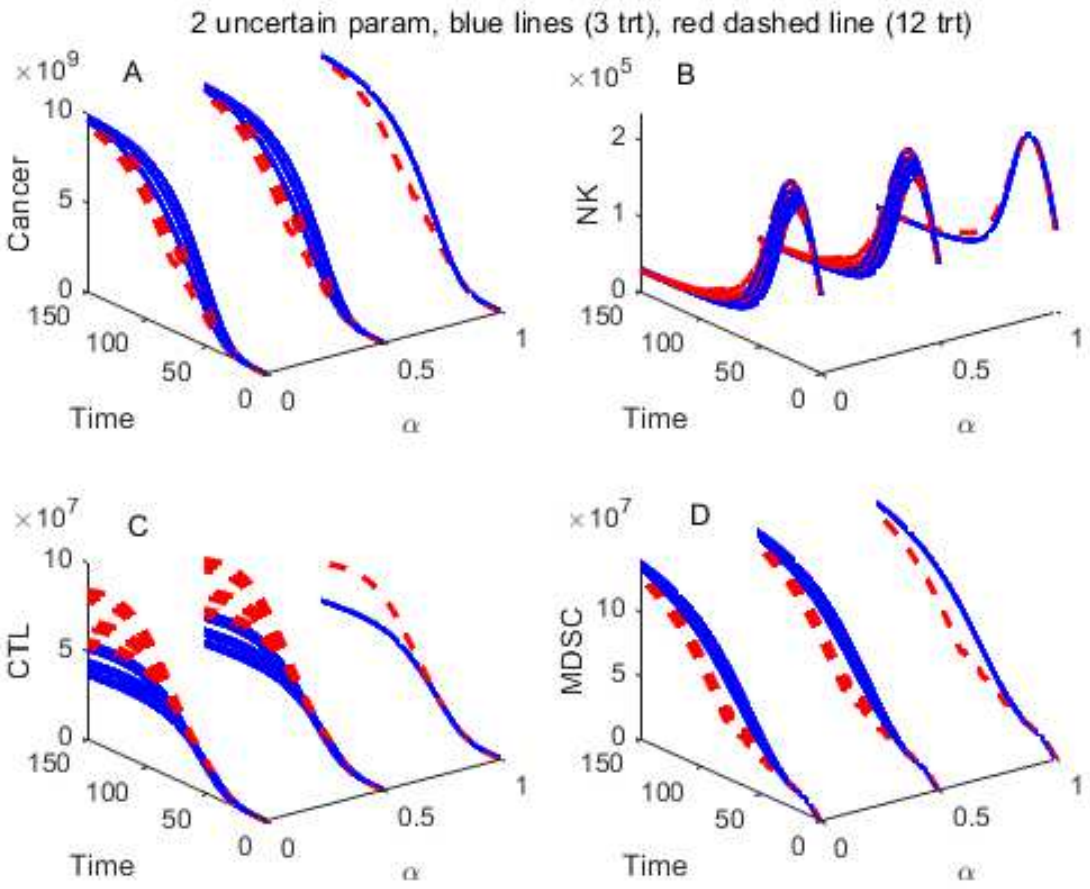

Figure 4. A three-dimensional simulation plot of cancer cells (A), NK cells (B), CTLs(C) and MDSCs (D) for two different timing of 5-FU treatment (same as those given in Figure 2) in fuzzy setting of kinetic parameters. The two fuzzy uncertain numbers are given as follow: $a = (0.9, 1, 1.1) \times 1.45 \times 10^{-1}$ and $f = (0.9, 1, 1.1) \times 4.12 \times 10^{-2}$.

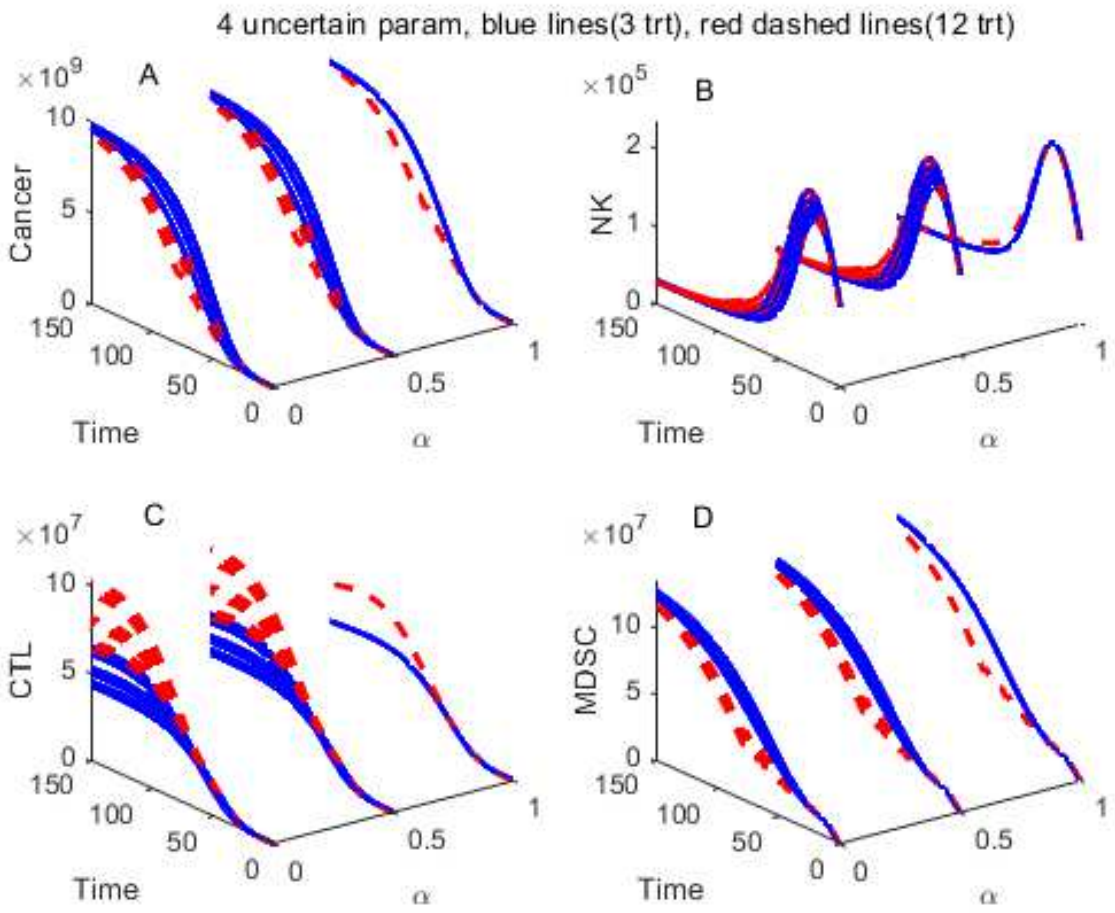

Figure 5. A three-dimensional simulation plot of cancer cells(A), NK cells (B), MDSCs (C) and CTLs (D) for two different timing of 5-FU treatment (same as those given in Figure 2) in fuzzy setting of kinetic parameters. The four fuzzy uncertain numbers are given as follow: $a = (0.9, 1, 1.1) \times 1.45 \times 10^{-1}$, $f = (0.9, 1, 1.1) \times 4.12 \times 10^{-2}$, $m = (0.9, 1, 1.1) \times 2 \times 10^{-2}$ and $\alpha = (09, 1, 1.1) \times 7 \times 10^{6}$.

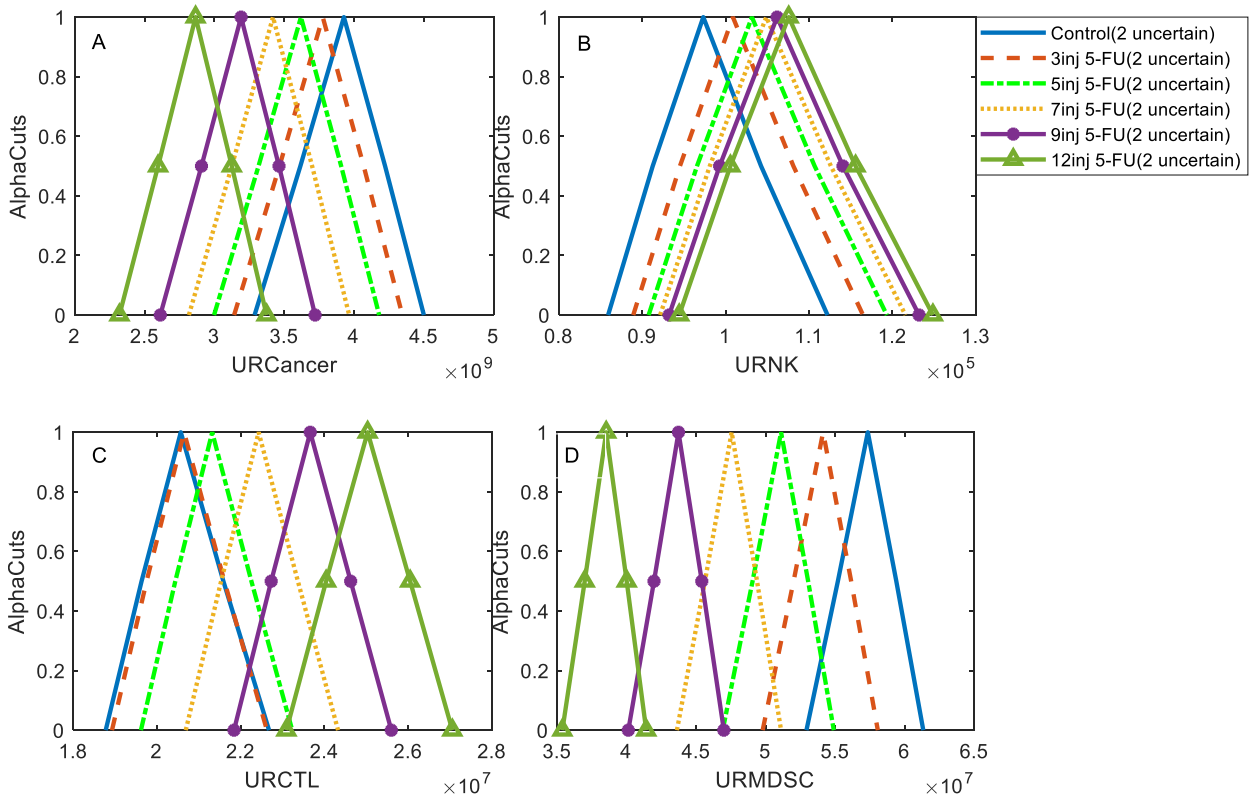

Figure 6. The membership function of average of dynamics of cancer cells (A), NK cells (B), CTLs(C) and MDSCs (D) in the time interval from day 10 to day 100 (after first 5-FU injection) for different timing of 5-FU injection (10:6:22, 10:6:34, 10:6:46, 10:6:58, 10:6:76) in fuzzy setting of kinetic parameters. The two fuzzy uncertain numbers are given as follow:

$a = (0.9, 1, 1.1) \times 1.45 \times 10^{-1}$ and $f = (0.9, 1, 1.1) \times 4.12 \times 10^{-2}$.

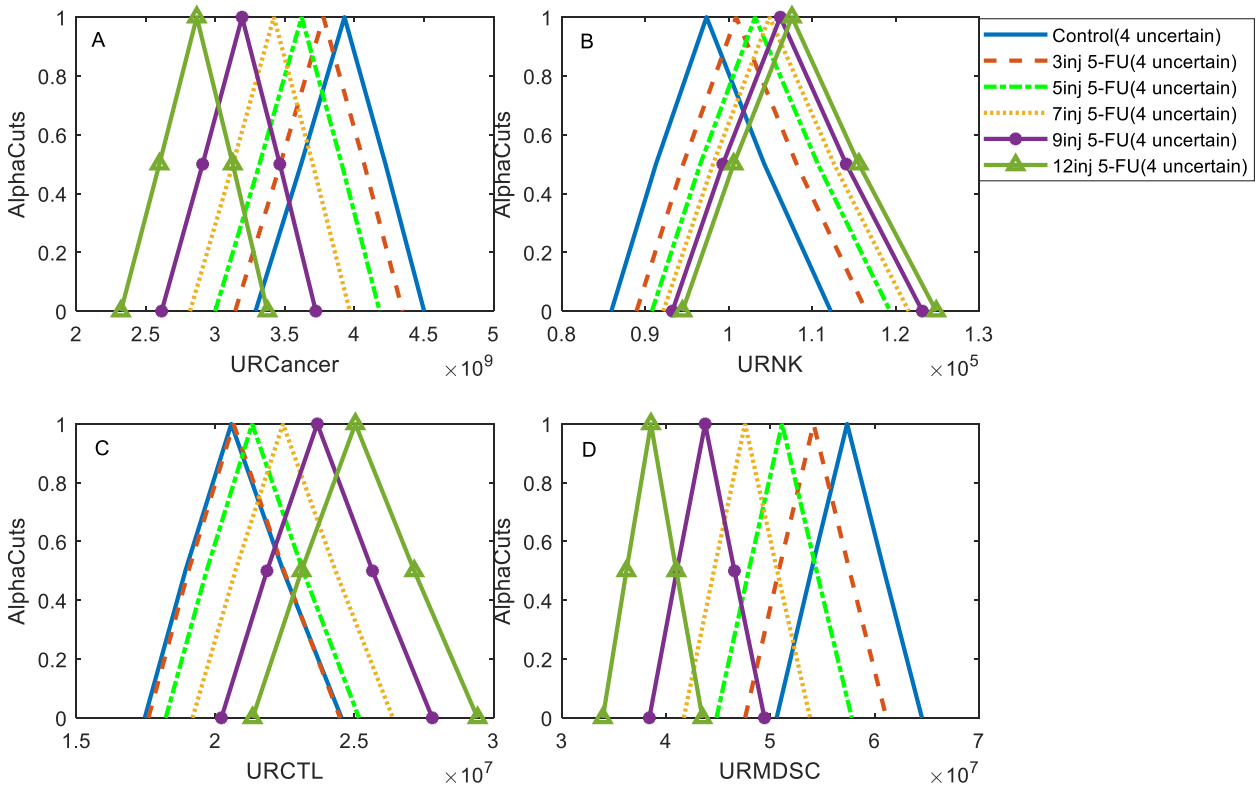

Figure 7. The membership function of average of dynamics of cancer cells (A), NK cells (B), CTLs(C) and MDSCs (D) in the time interval from day 10 to day 100 (after first 5-FU injection) for different timing of 5-FU injection (10:6:22, 10:6:34, 10:6:46, 10:6:58, 10:6:76) in fuzzy setting of kinetic parameters. The four fuzzy uncertain numbers are given as follow: $a = (0.9, 1, 1.1) \times 1.45 \times 10^{-1}$, $f = (0.9, 1, 1.1) \times 4.12 \times 10^{-2}$,$m = (0.9, 1, 1.1) \times 2 \times 10^{-2}$ and $\alpha = (09, 1, 1.1) \times 7 \times 10^{6}$.

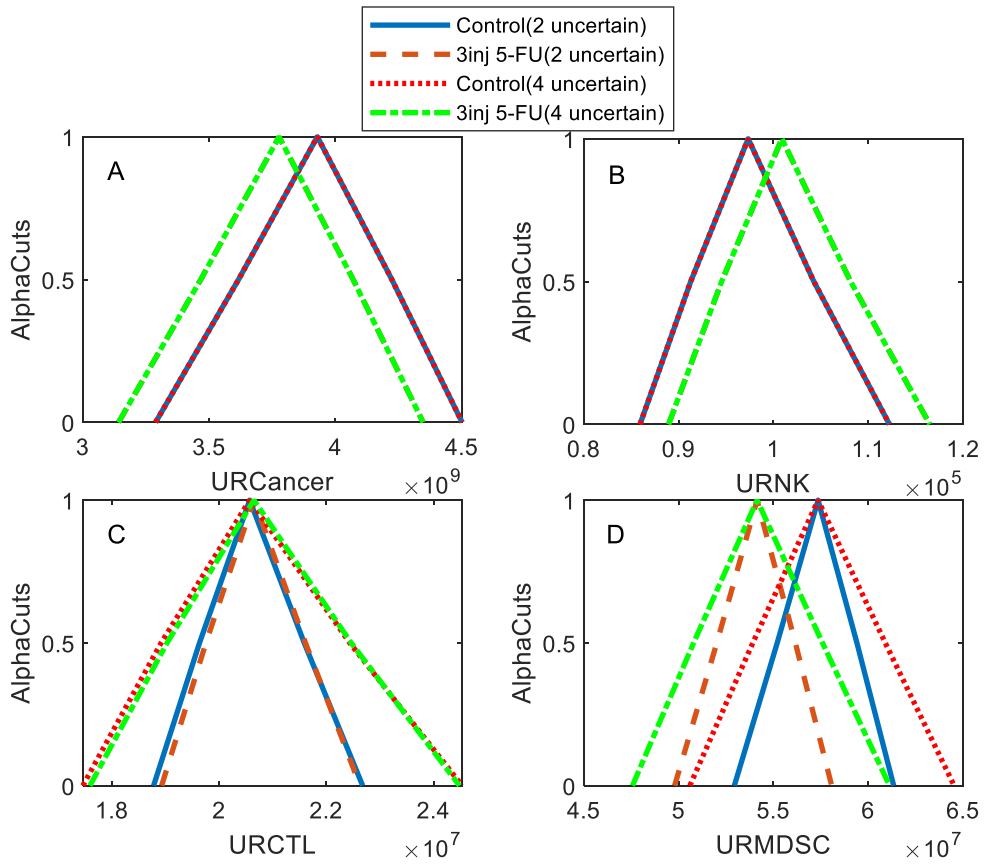

Figure 8. The membership function of average of dynamics of TIS' cells in the time interval from day 10 to day 100 (after first 5-FU injection) in control group (no treatment) and 5-FU treatment group (on day 10:6:22 after tumor inoculation) and in two different fuzzy settings (two or four fuzzy uncertain kinetic parameters). (A) shows the membership function of averaged dynamics of cancer cells in control compared with 5–FU treatment group and with regarding two fuzzy parameters (same as those given in figure 4) or four fuzzy parameters (same as those given in figure 5). (A), (B), (C) and (D) depict the membership function of averaged dynamics of cancer cells, NK cells, CTLs and MDSCs, respectively. The blue solid line depicts the membership function of fuzzy uncertain outcome measures (cancer cells, NK cells, CTLs and MDSCs) in control group (no treatment) with regarding two fuzzy uncertain kinetic parameters (same as figure 4), the brown dashed lines shows for 5-FU treatment (three times) and two fuzzy parameters, the red dotted line shows for control group and four fuzzy uncertain parameters, and green dash-dotted line depicts for 5-FU treatment (three times) and four uncertain parameters.

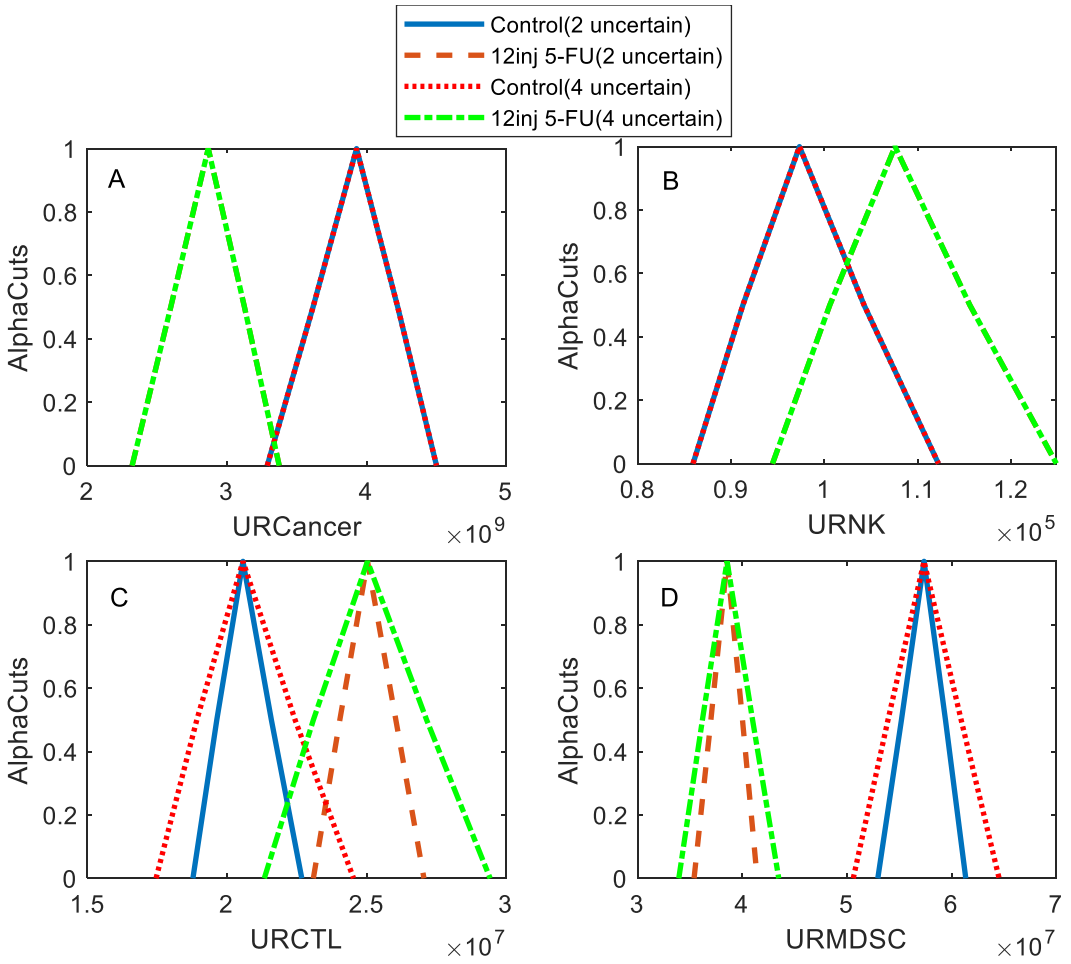

Figure 9. The membership function of average of dynamics of TIS' cells in the time interval from day 10 to day 100 (after first 5-FU injection) in control group (no treatment) and 5-FU treatment group (on day 10:6:76 after tumor inoculation) and in two different fuzzy settings (two or four fuzzy uncertain kinetic parameters). (A) shows the membership function of averaged dynamics of cancer cells in control compared with 5–FU treatment group and with regarding two fuzzy parameters (same as those given in figure 4) or four fuzzy parameters (same as those given in figure 5). (A), (B), (C) and (D) depict the membership function of averaged dynamics of cancer cells, NK cells, CTLs and MDSCs, respectively. The blue solid line depicts the membership function of fuzzy uncertain outcome measures (cancer cells, NK cells, CTLs and MDSCs) in control group (no treatment) with regarding two fuzzy uncertain kinetic parameters (same as figure 4), the brown dashed lines shows for 5-FU treatment (ten times) and two fuzzy parameters, the red dotted line shows for control group and four fuzzy uncertain parameters, and green dash-dotted line depicts for 5-FU treatment (ten times) and four uncertain parameters.

Global Sensitivity analysis:

Global sensitivity analysis (GSA) identify a few most influential kinetic parameters from a model with large number of parameters, which is critical for optimization and structural design. In this section, we perform global sensitivity analysis to investigate the impact of change in the models' kinetic parameters on dynamics of tumor cells, NK cells,

CTLs and MDSCs. To this end, we use partial rank correlation coefficient (PRCC) method to compute the correlation between outcome measures (population of cells) with respect to the all kinetic parameters of the model that are listed in table 1. Following sensitivity analysis developed in [51], we assign uniform distribution for all parameters of the model (in the range of one-half to twice its value in table 1) and generate 1000 samples from these distributions using Latin hypercube sampling (LHS). Then we evaluate the model by these samples (capture dynamics of TIS agent), then compute the PRCC values and the corresponding p-values (significance level) with respect to the dynamic of all cells at days 50, 100 and 200 of the model simulation and cells' average dynamics from day 0 to day 200.

The heatmaps related to the global sensitivity analysis include the mean and standard deviation of the PRCC values (five replication) and the corresponding p-values (maximum of p-values for five replication). The first panel of figures 10, 11, 12 and 13 illustrate the 5 replicated average of PRCC values for cells (cancer cells, NK cells, CTLs and MDSCs) populations' record on days 50, 100, 200 after tumor inoculation and for average of dynamics of cells in the time interval from day 0 to day 200, respectively. The second and third panel of figures 10, 11, 12 and 13 depicted the standard deviation of PRCC values for 5 replication and corresponding p-values (maximum of p-values for 5 replication) for record of cell populations on days 50, 100, 200 after tumor inoculation and for average of dynamics of cells in the time interval from day 0 to day 200, respectively. Each pixel shows the correlation between the population of cells (on the vertical axis) and kinetic parameters (on the horizontal axis). Correlation values range from -1 to +1 and measures linear trend between two variables (population of cell and kinetic parameter). In Figures 10, 11, 12 and 13, only meaningful correlation values (p-value<0.05) are presented.

As depicted in Figure 10.A, there is a strong correlation between the population of cancer cells at day 50 and parameters a (growth rate of cancer cells) and $Cmax$ (carrying capacity of tumor). Also, population of MDSCs at day 50 and parameters $a, Cmax$ have same correlation. As it's depicted, there is a negative correlation between population of NK cells (and also CTLs) and parameters $a, Cmax$ and l (depth of access of immune cells to tumor cells). Also, there is a positive correlation between population of NK cells at day 50 and parameter σ (constant influx rate of NK cells following encounter with tumor cells). There is a negative correlation between the population of NK cells at day 50 and parameter p (inactivation rate of NK cells) and also between population of CTLs at same time and parameter m (death rate of CTLs). Results of PRCC analysis show that there is an inverse correlation between the population of cancer cells (and also MDSCs) at day 50 and parameter j (maximum recruitment rate of CTLs), while there is a positive correlation between the population of CTLs (and also NK cells) with this parameter. As it's showed, population of MDSCs at day 50 has a positive correlation with parameters α (MDSC's expansion rate),ρ (MDSC's production rate) and also has an inverse correlation with β (MDSC's apoptosis rate),q (Steepness coefficient of the MDSCs production curve). The results of PRCC analysis revealed that the population of CTLs at day 50 has an inverse correlation with parameter v (differentiation rate of CTLs into other types of T cells such as Treg).

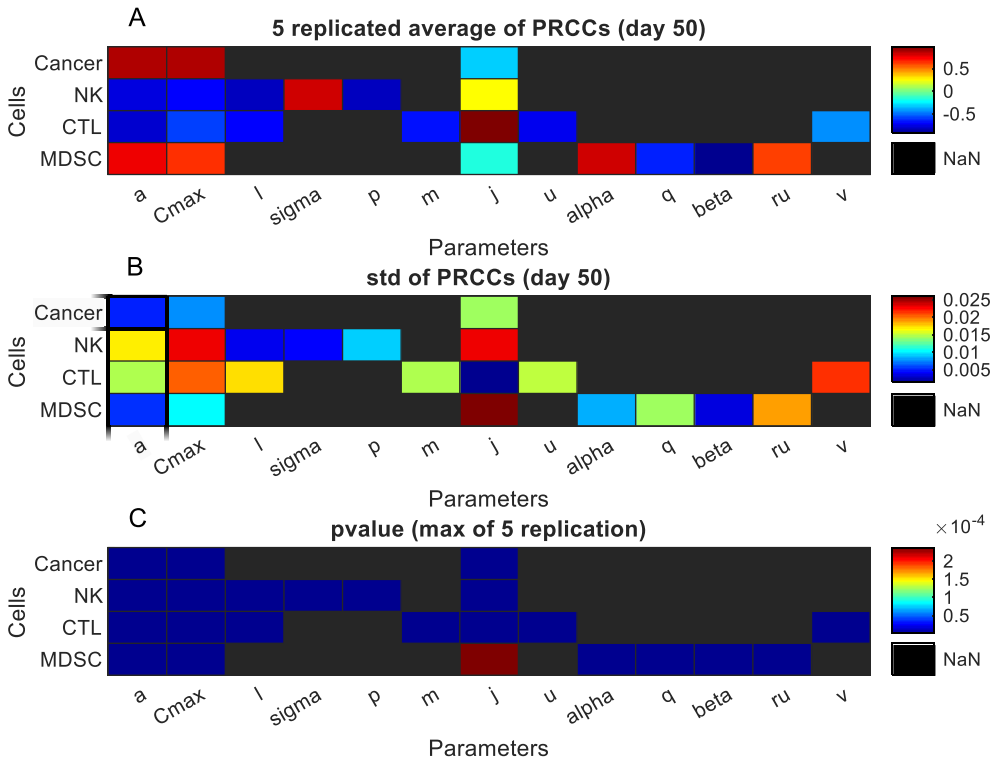

Figure 10. Statistically significant PRCC values (p-value<0.05) for tumor cells, NK cells, CTLs and MDSCs at day 50 after tumor injection. The first and second panels show the mean and standard deviation of PRCC values for five replications of PRCC analysis and the third panel depicts the maximum of their corresponding p-values. Black pixels (NaN) show 'not a number' and represent no significant correlation between outcome measures (population of cells, elements in vertical axis) and kinetic parameters of model (elements in horizontal axis).

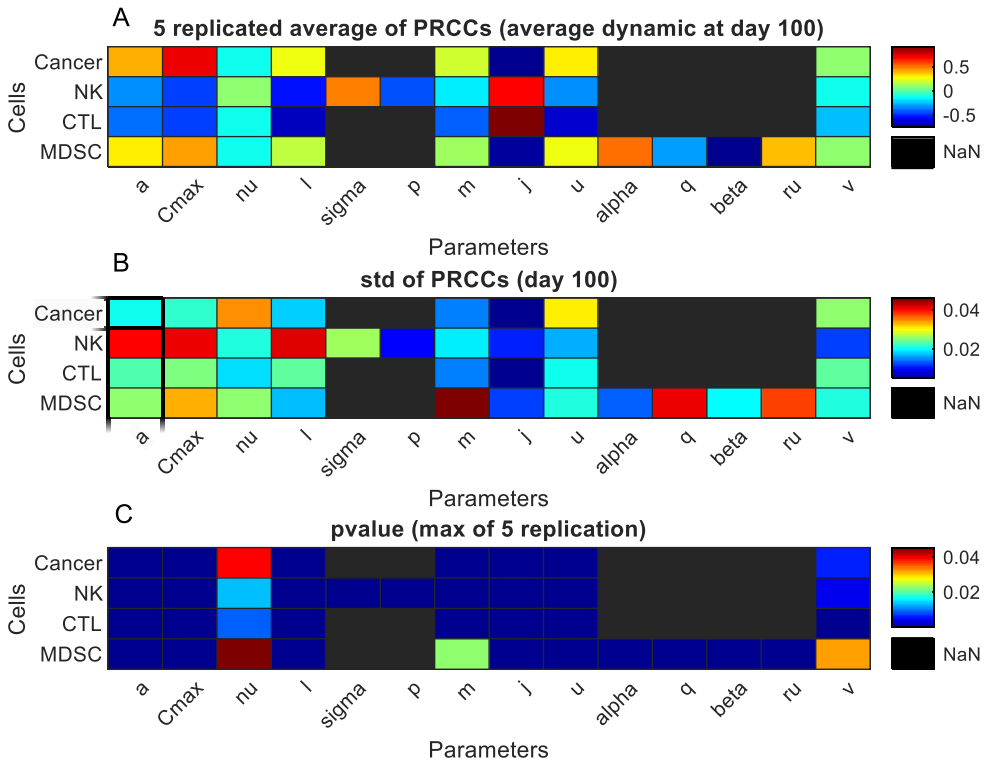

Figure 11. Statistically significant PRCC values (p-value<0.05) for tumor cells, NK cells, CTLs and MDSCs at day 100 after tumor injection. The first and second panels show the mean and standard deviation of PRCC values for five replications (or five replicates) of PRCC analysis and the third panel depicts the maximum of PRCC corresponding p-values. Black pixels (NaN) shows 'not a number' and represents no significant correlation between outcome measures (population of cells, its element in vertical axis) and kinetic parameters of model (element in horizontal axis).

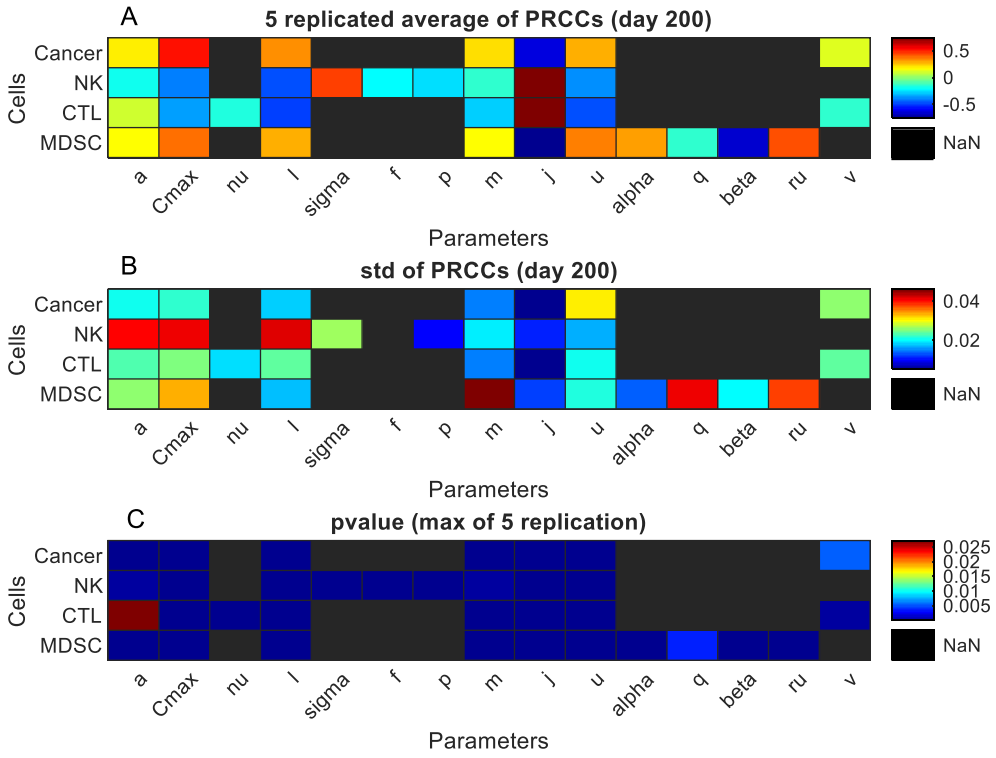

Figure 12. Statistically significant PRCC values (p-value<0.05) for tumor cells, NK cells, CTLs and MDSCs at day 200 after tumor injection. The first and second panels show the mean and standard deviation of PRCC values for five replication or five replicates of PRCC analysis and the third panel depicts the maximum of PRCC corresponding p-values. Black pixels (NaN) shows 'not a number' and represents no significant correlation between outcome measures (population of cells, elements in vertical axis) and kinetic parameters of model (element in horizontal axis).

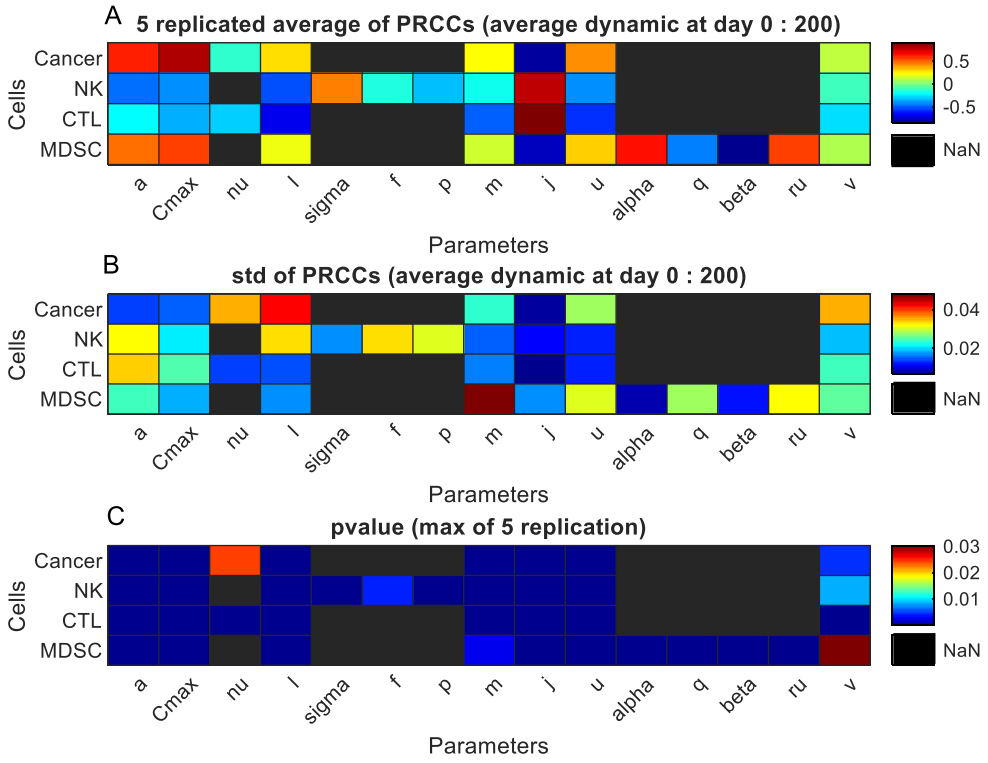

Figure 13. Statistically significant PRCC values (p-value<0.05) for an average of dynamics of tumor cells, NK cells, CTLs and MDSCs in the time interval from day 0 to day 200 after tumor injection. The first and second panels show the mean and standard deviation of PRCC values for five replications of PRCC analysis and the third panel depicts the maximum of PRCC corresponding p-values. Black pixels (NaN) shows 'not a number' and represents no significant correlation between outcome measures (population of cells, elements in vertical axis) and kinetic parameters of model (element in horizontal axis).

In this section we aim to by elementary effects test identify which of kinetic parameters have nonlinear or linear effects[52]. Morris GSA used to screen and identify which of 22 kinetic parameters of model are most influential and have significant effect on outcome measures (cell's dynamics). For 22 kinetic parameters, elementary effects test using Morris sampling strategy were taken into account by setting 6 levels in the sampling grid and 1000 trajectories to compute the mean μ^* and standard deviation σ. The identified most influential kinetic parameters with respect to the mean $\mu^*$and interaction effect σ are depicted in figure 14. The parameters with large σ values indicate nonlinear and interaction effects, while the parameters with largeμ^*values indicate the linear or additive effects. The dashed line $\mu^* = \frac{2\sigma}{sqrt(r)}$ (r is number of trajectories) which all parameters are below that, translates into 95% confidence interval.

Morris analysis was performed by considering the mean population of tumor cells, NK cells, CTLs and MDSCs (in no treatment case) from day 0 to day 100 of simulation as read-out. The results of the sensitivity analysis with 10% perturbations showed in figure 14. Our findings revealed that the parameters a, $Cmax$ and b, reflecting the tumor

growth rate, carrying capacity or maximal population of tumor cells, and NK cell-mediated tumor cell killing rate, respectively, were identified as being important for the tumor cell output (Figure 14.A). The parameters b has most interaction effect, while the parameter a has most linear effect on dynamics of tumor cells.

The parameters a, $Cmax$, b and η(CTL-mediated tumor killing rate), were predicted to play an important role in the regulation of NK cells population and all of them have the most interaction and linear effects (Figure 14.B). The parameter a is the most influential parameter on man population of CTLs and has most interaction and linear effects (Figure14.C).The parameters a, $Cmax$, b, η and l(depth of access of immune cells to tumor cells) were identified as most influential kinetic parameters for the mean of MDSCs from day 0 to day 100 of simulation and all of these parameters have interaction and linear effect for MDSCs (Figure 14.D).

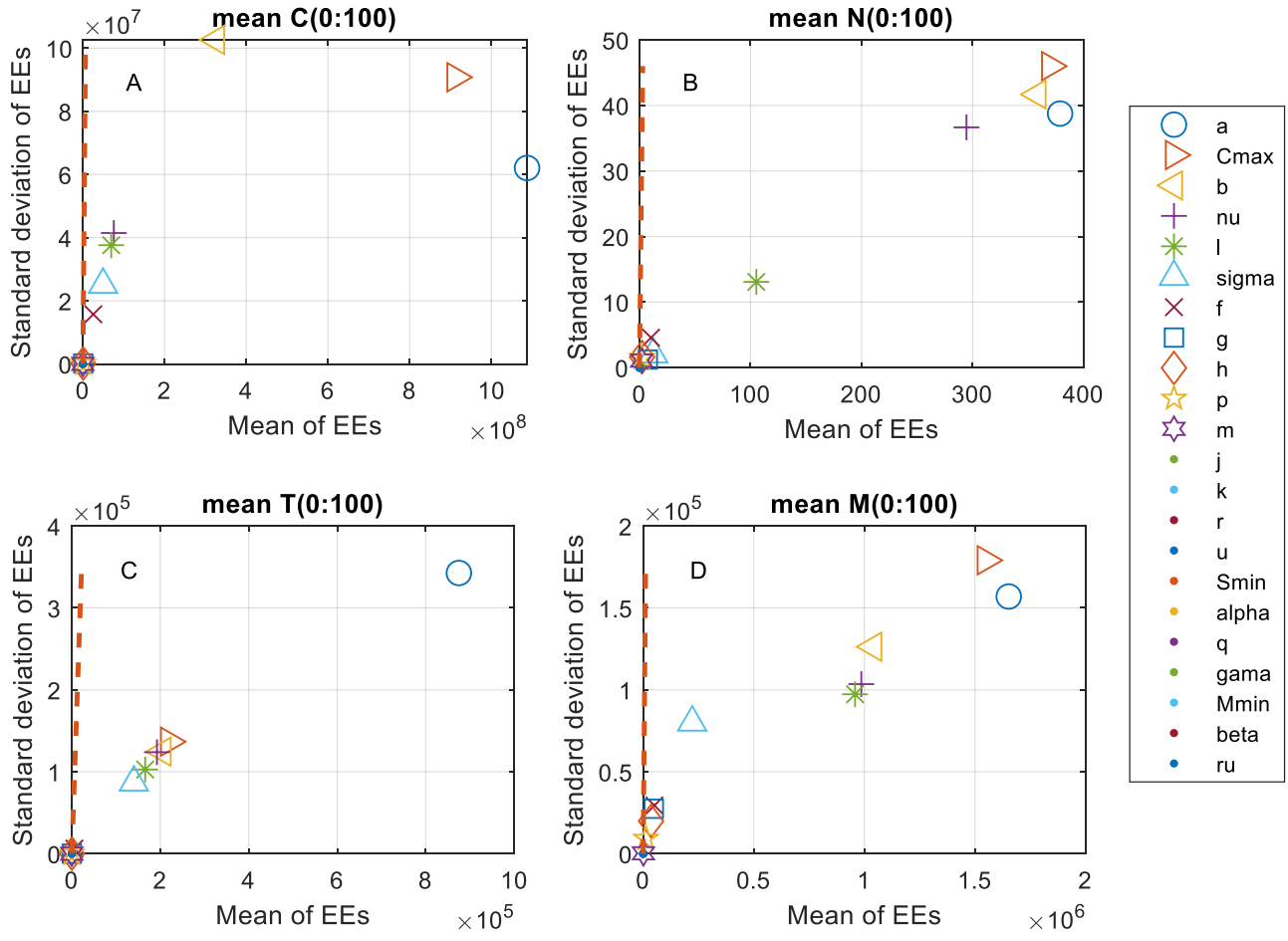

Figure 14. The absolute mean value and standard deviation of Morris GSA (elementary effects analysis). Figures present the relative importance of kinetic parameters of TIS model, considering the mean population of tumor cells (A), mean population of NK cells (B), mean population of CTLs (C) and mean population of MDSCs (D) from day

0 to day 100 as read-out. Each kinetic parameter is specified by two Morris indices, σ (vertical axis) and μ^*(horizontal axis), which describe the interaction or nonlinear effects and the significance of the effects, respectively.

Conclusion:

In this study, we aimed to capture the uncertainty of kinetic parameters of an ODE model of tumor-immune system (TIS). The ODE model of TIS mechanistically models the interactions of tumor cells, CTLs, NKs and MDSCs. CTLs and NK cells are the most important cells of adaptive and innate immune system, respectively that encounter with tumor cells, while MDSCs as immature immune cells suppress the immune responses in the inflammatory environments. To capture uncertainty of parameters of ODE model, fuzzy theorem has been used and fuzzy numbers assigned with specific membership functions (triangular) instead of crisp numbers to the kinetic parameters of ODE model to capture the uncertainty of outcome measures (population of TIS agents or cells) as a result of the uncertainties of the parameters. Therefore, the uncertainty source of TIS agents' dynamics is uncertainty of the model's kinetic parameters. The source of uncertainty of kinetic parameters is error in experimental data, missing or incomplete data. Also, some features of TIS causes the kinetic/dynamic rate of different actions, behaviors, and interaction of system to be uncertain, including, variability and dynamics of TIS from patient to patient and during time and treatment, dynamical features of TIS including dynamic cell size, cell density, various and unpredictable patterns of extracellular ligands and receptors, evolutionary mutation types during time and treatment, diversity in phenotypic patterns, chaotic and complex patterns of vasculature status, etc. All of these features make the TIS a complex system, requires very sophisticated mathematical functions and many kinetic parameters that must be estimated by imprecise in vitro/in vivo data. For the sake of brevity and simplicity of mathematical model, we propose using of ODE model with fuzzy uncertain kinetic parameters to construct a fuzzy ordinary differential equation (FODE) model. FODE model can be used for the dynamic analysis of the TIS interactions and in silico assessment of 5-FU chemotherapy to suppress MDSCs and tumor cells. By simulating different cell behaviors and through mechanistically modeling the different immune-tumor cells interactions, the FODE model predicts the dynamics of cells. The model also simulates the effect of 5-FU treatment for the improvement of the immune system performance in the inflammatory environment. The FODE is configurable for 5-FU chemotherapy injection timing and was used to investigate the efficacy of 5-FU chemotherapy in the fuzzy setting. Simulations results revealed that 5-FU therapy caused the uncertainty band of the population of cancer cells and MDSCs to shift to the smaller populations while the uncertainty band of the population of NK cells and CTLs shifted to the larger populations. Our data reveals that increasing/decreasing the uncertainty band of the model's fuzzy parameters increases/decreases the uncertainty region of dynamics of species. We concluded that 5-FU therapy limits tumor growth and induces anti-tumor immunity. Since fuzzy analysis takes into account parametric uncertainty of TIS, in silico assessment of 5-FU therapy in fuzzy setting generates robust suggestions for the protocol of 5-FU treatment in vitro/in vivo or clinical trial.

The results of the model simulations with 5-FU injection are qualitatively consistent with that results of in vivo studies[10][48][49]. Besides, to help understand the mechanisms of tumor-immune system interactions, the model can

also provide testable hypotheses in vitro/in vivo experiments. So that the model can be developed via in vitro/in vivo data and parameterized (learned) model can be evaluated in silico environment and model refinement can be done through in vivo/in silico (or in vitro/in silico) iterative process. Regarding the dynamic information obtained from in silico experiments, a more detailed study of the system can be conducted in vitro/in vivo experiments.

Discussion:

One of the major challenges in the field of mathematical oncology is the lack of sufficient precise empirical data (in vitro/ in vivo) for model parameterization and estimating crisp values for parameters. The high sensitivity of differential equation models to kinetic parameters caused the model calibration to be a difficult task. Models such as Petri nets, Agent-based models, Boolean networks, and the cellular automata models have less kinetic parameters compared to the differential equation models. Whereas in differential equation models, many parameters are required to model different behaviors of the system. This matter causes the models based on differential equations to encounter major limitations when they are used to model the systems with insufficient imprecise experimental data. While kinetic parameters' fuzzification in differential equation models eliminates such limitations.

The ODE model of TIS of this study is taken from [40]which is parameterized by imprecise in vivo data sets from different cell lines including EL4-luc2 (murine lymphoma cancer cell line), 4T1 (murine breast cancer cell line) and 3LL (murine lung cancer cell line). In this study, we aimed to reconstruct this ODE model with fuzzy theorem to capture fuzzy uncertainty of kinetic parameters. Due to error in data acquisition, inaccurate, incomplete or missing data, natural variability between patients and variable environmental factors, etc., the kinetic parameters of TIS are uncertain and assigning a fuzzy numbers instead of a crisp values, can help us to capture uncertainty band of tumor and immune cells (compose the membership function of cells as a result of uncertainty of kinetic parameters). Therefore, this study presents the procedure of fuzzification of kinetic parameters of ODE models and although it is illustrated for the ODE model of TIS but is not confined to this system and can be used for any ODE model.

Uncertainty as an inherent feature of biological systems should be considered in computational models. There is two types of uncertainty, randomness and fuzziness. Random uncertainty is simulated using stochastic models such as stochastic Petri net, stochastic differential equations, agent-based models with stochastic rules, probabilistic Boolean networks, Markov model, etc. The stochastic differential equations (SDEs) with random parameters belonging to specific probability density functions (PDFs), create stochastic perturbation terms. By sampling the PDFs of the parameters, and simulating the model with random parameters, the dynamic uncertainty band of the model components (cells) is obtained. In present study, we analyzed the effect of randomness of kinetic parameters through global sensitivity analysis (GSA). In GSA, we performed elementary effect (EE) test[52] and partial rank correlation coefficient (PRCC) test [51] that by Morris sampling and by Latin hypercube sampling strategies, respectively, from uniform distribution of parameters, execute ODE model of TIS (with sampled parameters) and quantify the dynamical behavior of cells. In present study, we wanted to quantify the effect of fuzziness of kinetic parameters, therefore we designed a fuzzy ODE model. The ODE model with fuzzy kinetic parameters creates a framework to include the quantities with imprecise values. In FODE, we decompose the membership function of kinetic parameters into its α-cuts and discretize each α-cut to different levels and execute ODE model with that parameters to compose α-cuts of

cell's dynamics (to form membership function of cells' dynamics). This fuzzification method of kinetic parameters is similar with that used in stochastic petri net [38][53] and continuous petri net[39].

Using the present model, researchers can test different hypotheses by in silico experiments. Also, they can predict the dynamics of different behaviors/interactions of TIS through the nonlinear complex FODE model. The results of chemotherapy by 5-FU injection can provide a practical tool for the medical community to conduct experiments in the laboratory environment. Finally, we need to point out that even though the fuzzification method for ODE parameters described in this study has been used in a TIS model, but it is not confined to this system and as a powerful tool can be applied to ODE model of any biological network. In silico design of 5-FU treatment conducted by novel FODE model help us to test different schedules of this treatment by virtual clinical therapy and also significantly reduce the cost.

Data accessibility.

MATLAB code and description of GUI is available in the electronic supplementary material.

Ethics.

Since this study was the mathematical modeling using the findings of the other published articles, no ethical approval was necessary.

Competing interests.

We have no competing interests.

Funding.

This work partially was supported by a grant from the Tehran University of Medical Sciences (TUMS)

Author Contributions:

Conceptualization, all authors; Methodology and software, SS; Formal analysis, SS; Investigation, all authors; Writing – Original Draft, SS; Writing – Review & Editing, all authors; Visualization, SS; Supervision, NGH. All authors read and approved the final manuscript.

Acknowledgments.

This work was supported by the Qazvin University of Medical Sciences grants…. The authors thank Philip Maini and Roobina Boghozian for critical comments on the manuscript.

Conflicts of Interest.

The authors declare no conflict of interest.

References.

[1] "Worldwide cancer statistics | Cancer Research UK." https://www.cancerresearchuk.org/health-professional/cancer-statistics/worldwide-cancer (accessed Apr. 03, 2020).

[2] A. Abbas, A. Lichtman, and S. Pillai, *Cellular and molecular immunology E-Book*. 2011.

[3] T. Gajewski, H. Schreiber, Y. F.-N. immunology, and undefined 2013, "Innate and adaptive immune cells in the tumor microenvironment," *nature.com*, Accessed: Apr. 02, 2020. [Online]. Available: https://www.nature.com/articles/ni.2703.

[4] C. Guillerey, N. Huntington, M. S.-N. immunology, and undefined 2016, "Targeting natural killer cells in cancer immunotherapy," *nature.com*, Accessed: Apr. 02, 2020. [Online]. Available: https://www.nature.com/ni/journal/v17/n9/abs/ni.3518.html.

[5] K. Parker, D. Beury, S. O.-R.-A. in cancer, and undefined 2015, "Myeloid-derived suppressor cells: critical cells driving immune suppression in the tumor microenvironment," *Elsevier*, Accessed: Apr. 02, 2020. [Online]. Available: https://www.sciencedirect.com/science/article/pii/S0065230X15000305.

[6] C. Liu, C. J. Workman, and D. A. A. Vignali, "Targeting regulatory T cells in tumors," *FEBS Journal*. Blackwell Publishing Ltd, pp. 2731–2748, Jul. 01, 2016, doi: 10.1111/febs.13656.

[7] C. Groth, X. Hu, R. Weber, V. Fleming, … P. A.-B. journal of, and undefined 2019, "Immunosuppression mediated by myeloid-derived suppressor cells (MDSCs) during tumour progression," *nature.com*, Accessed: Apr. 02, 2020. [Online]. Available: https://www.nature.com/articles/s41416-018-0333-1.

[8] R. T.-T. in pharmacological sciences and undefined 2019, "MDSC; the most important cell you have never heard of," *Elsevier*, Accessed: Apr. 02, 2020. [Online]. Available: https://www.sciencedirect.com/science/article/pii/S0165614718301895.

[9] M. Munder, H. Schneider, C. Luckner, T. G.- Blood, and undefined 2006, "Suppression of T-cell functions by human granulocyte arginase," *ashpublications.org*, Accessed: Apr. 02, 2020. [Online]. Available: https://ashpublications.org/blood/article-abstract/108/5/1627/132630.

[10] M. Abedi-Valugerdi, J. Wolfsberger, … P. P.-I., and undefined 2016, "Suppressive effects of low-

dose 5-fluorouracil, busulfan or treosulfan on the expansion of circulatory neutrophils and myeloid derived immunosuppressor cells in," *Elsevier*, Accessed: Apr. 02, 2020. [Online]. Available: https://www.sciencedirect.com/science/article/pii/S1567576916303411.

[11] A. K. Nowak, B. W. S. Robinson, and R. A. Lake, "Gemcitabine Exerts a Selective Effect on the Humoral Immune Response: Implications for Combination Chemo-immunotherapy 1," 2002. Accessed: Apr. 02, 2020. [Online]. Available: https://cancerres.aacrjournals.org/content/62/8/2353.short.

[12] V. Umansky, C. Blattner, C. Gebhardt, and J. Utikal, "The Role of Myeloid-Derived Suppressor Cells (MDSC) in Cancer Progression," *mdpi.com*, doi: 10.3390/vaccines4040036.

[13] M. K. Srivastava *et al.*, "Myeloid suppressor cell depletion augments antitumor activity in lung cancer," *PLoS One*, vol. 7, no. 7, Jul. 2012, doi: 10.1371/journal.pone.0040677.

[14] J. Vincent *et al.*, "5-Fluorouracil Selectively Kills Tumor-Associated Myeloid-Derived Suppressor Cells Resulting in Enhanced T Cell-Dependent Antitumor Immunity," *AACR*, 2010, doi: 10.1158/0008-5472.CAN-09-3690.

[15] Y. Si, S. Merz, P. Jansen, … B. W.-S., and undefined 2019, "Multidimensional imaging provides evidence for down-regulation of T cell effector function by MDSC in human cancer tissue," *immunology.sciencemag.org*, Accessed: Apr. 02, 2020. [Online]. Available: https://immunology.sciencemag.org/content/4/40/eaaw9159.abstract.

[16] V. Anagnostou *et al.*, "Dynamics of Tumor and Immune Responses during Immune Checkpoint Blockade in Non-Small Cell Lung Cancer," *AACR*, 2019, doi: 10.1158/0008-5472.CAN-18-1127.

[17] Q. Zhang *et al.*, "Landscape and dynamics of single immune cells in hepatocellular carcinoma," *Elsevier*, Accessed: Apr. 02, 2020. [Online]. Available: https://www.sciencedirect.com/science/article/pii/S0092867419311195.

[18] S. Felts, X. Tang, B. Willett, … V. V. K.-C., and undefined 2019, "Stochastic changes in gene expression promote chaotic dysregulation of homeostasis in clonal breast tumors," *nature.com*, Accessed: Apr. 02, 2020. [Online]. Available: https://www.nature.com/articles/s42003-019-0460-0.

[19] K.-A. Norton, C. Gong, S. Jamalian, and A. S. Popel, "Multiscale Agent-Based and Hybrid Modeling

of the Tumor Immune Microenvironment," *mdpi.com*, doi: 10.3390/pr7010037.

[20] G. Mahlbacher, K. Reihmer, H. F.-J. of theoretical biology, and undefined 2019, "Mathematical modeling of tumor-immune cell interactions," *Elsevier*, Accessed: Apr. 02, 2020. [Online]. Available: https://www.sciencedirect.com/science/article/pii/S0022519319300955.

[21] J. G. da Silva, R. M. de Morais, I. C. R. da Silva, and P. F. de Arruda Mancera, "Mathematical models applied to thyroid cancer," *Biophysical Reviews*, vol. 11, no. 2. Springer Verlag, pp. 183–189, Apr. 01, 2019, doi: 10.1007/s12551-019-00504-7.

[22] F. Bianconi, C. Antonini, L. Tomassoni, and P. Valigi, "An application of Conditional Robust Calibration (CRC) to ordinary differential equations (ODEs) models in computational systems biology: a comparison of two sampling strategies," *IET Syst. Biol.*, 2019, doi: 10.1049/iet-syb.2018.5091.

[23] A. d'Onofrio-M. and C. Modelling and undefined 2008, "Metamodeling tumor–immune system interaction, tumor evasion and immunotherapy," *Elsevier*, Accessed: Apr. 03, 2020. [Online]. Available: https://www.sciencedirect.com/science/article/pii/S0895717707001951.

[24] L. G. de Pillis, A. E. Radunskaya, and C. L. Wiseman, "A validated mathematical model of cell-mediated immune response to tumor growth," *Cancer Res.*, vol. 65, no. 17, pp. 7950–7958, 2005.

[25] K. J. Mahasa, R. Ouifki, A. Eladdadi, and L. de Pillis, "Mathematical model of tumor–immune surveillance," *J. Theor. Biol.*, vol. 404, pp. 312–330, 2016.

[26] N. Moore, D. Doty, M. Zielstorff, I. Kariv, L. M.-L. on a Chip, and undefined 2018, "A multiplexed microfluidic system for evaluation of dynamics of immune–tumor interactions," *pubs.rsc.org*, Accessed: Apr. 02, 2020. [Online]. Available: https://pubs.rsc.org/--/content/articlehtml/2018/lc/c8lc00256h.

[27] F. A. Rihan *et al.*, "Dynamics of tumor-immune system with fractional-order," *J. Tumor Res.*, vol. 2, no. 1, pp. 109–115, 2016.

[28] A. Hara and Y. Iwasa, "Coupled dynamics of intestinal microbiome and immune system—A mathematical study," *J. Theor. Biol.*, vol. 464, pp. 9–20, 2019.

[29] A. Allahverdy *et al.*, "An agent-based model for investigating the effect of myeloid-derived suppressor cells and its depletion on tumor immune surveillance," *J. Med. Signals Sens.*, vol. 9,

no. 1, 2019, doi: 10.4103/jmss.JMSS_33_18.

[30] C. Gong *et al.*, "A computational multiscale agent-based model for simulating spatio-temporal tumour immune response to PD1 and PDL1 inhibition," *J. R. Soc. Interface*, vol. 14, no. 134, p. 20170320, 2017.

[31] D. G. Mallet and L. G. De Pillis, "A cellular automata model of tumor–immune system interactions," *J. Theor. Biol.*, vol. 239, no. 3, pp. 334–350, 2006.

[32] F. Akbarian, S. Rahbar, S. Shafiekhani, A. H. Jafari, and J. Hajati, "Modeling the strategies of interactions between melanoma tumor and CD8+ immune cells using game theory," in *2018 25th National and 3rd International Iranian Conference on Biomedical Engineering (ICBME)*, 2018, pp. 1–4.

[33] M. L. Puri, D. A. Ralescu, and L. Zadeh, "Fuzzy random variables," in *Readings in fuzzy sets for intelligent systems*, Elsevier, 1993, pp. 265–271.

[34] S. Shafiekhani, A. Poursheykhani, S. Rahbar, and A. H. Jafari, "Simulating ATO Mechanism and EGFR Signaling with Fuzzy Logic and Petri Net," *J. Biomed. Phys. Eng.*, 2018.

[35] M. K. Morris, J. Saez-Rodriguez, D. C. Clarke, P. K. Sorger, and D. A. Lauffenburger, "Training signaling pathway maps to biochemical data with constrained fuzzy logic: quantitative analysis of liver cell responses to inflammatory stimuli," *PLoS Comput. Biol.*, vol. 7, no. 3, 2011.

[36] F. Liu, M. Heiner, and D. Gilbert, "Fuzzy Petri nets for modelling of uncertain biological systems," *Brief. Bioinform.*, vol. 21, no. 1, pp. 198–210, 2020.

[37] I. Park, D. Na, D. Lee, and K. H. Lee, "Fuzzy continuous Petri Net-based approach for modeling immune systems," in *Neural Nets*, Springer, 2005, pp. 278–285.

[38] F. Liu, M. Heiner, and M. Yang, "Fuzzy stochastic petri nets for modeling biological systems with uncertain kinetic parameters," *PLoS One*, vol. 11, no. 2, Feb. 2016, doi: 10.1371/journal.pone.0149674.

[39] F. Liu, S. Chen, M. Heiner, and H. Song, "Modeling biological systems with uncertain kinetic data using fuzzy continuous Petri nets," *BMC Syst. Biol.*, vol. 12, no. 4, pp. 63–74, Apr. 2018, doi: 10.1186/s12918-018-0568-8.

[40] S. Shariatpanahi, … S. S.-J. of theoretical, and undefined 2018, "Mathematical modeling of

tumor-induced immunosuppression by myeloid-derived suppressor cells: Implications for therapeutic targeting strategies," *Elsevier*, Accessed: Apr. 03, 2020. [Online]. Available: https://www.sciencedirect.com/science/article/pii/S0022519318300067.

[41] R. Serre *et al.*, "Mathematical modeling of cancer immunotherapy and its synergy with radiotherapy," *Cancer Res.*, vol. 76, no. 17, pp. 4931–4940, 2016.

[42] X. Lai and A. Friedman, "Combination therapy of cancer with cancer vaccine and immune checkpoint inhibitors: a mathematical model," *PLoS One*, vol. 12, no. 5, 2017.

[43] O. Milberg *et al.*, "A QSP Model for Predicting Clinical Responses to Monotherapy, Combination and Sequential Therapy Following CTLA-4, PD-1, and PD-L1 Checkpoint Blockade," *Sci. Rep.*, vol. 9, no. 1, pp. 1–17, 2019.

[44] J. Noorbakhsh and J. H. Chuang, "Uncertainties in tumor allele frequencies limit power to infer evolutionary pressures," *Nat. Genet.*, vol. 49, no. 9, p. 1288, 2017.

[45] N. Eling, M. D. Morgan, and J. C. Marioni, "Challenges in measuring and understanding biological noise," *Nat. Rev. Genet.*, vol. 20, no. 9, pp. 536–548, 2019.

[46] S. Wilson and D. Levy, "A Mathematical Model of the Enhancement of Tumor Vaccine Efficacy by Immunotherapy," *Bull. Math. Biol.*, vol. 74, no. 7, pp. 1485–1500, Jul. 2012, doi: 10.1007/s11538-012-9722-4.

[47] C. Twyman-Saint Victor *et al.*, "Radiation and dual checkpoint blockade activate non-redundant immune mechanisms in cancer," *Nature*, vol. 520, no. 7547, pp. 373–377, 2015.

[48] N. Werthmöller, B. Frey, M. Rückert, M. Lotter, R. Fietkau, and U. S. Gaipl, "Combination of ionising radiation with hyperthermia increases the immunogenic potential of B16-F10 melanoma cells in vitro and in vivo," *Int. J. Hyperth.*, vol. 32, no. 1, pp. 23–30, Jan. 2016, doi: 10.3109/02656736.2015.1106011.

[49] S. Orecchioni, G. Talarico, V. Labanca, and P. Mancuso, "Vinorelbine, cyclophosphamide, and 5-FU effects on the circulating and intratumoral landscape of immune cells improve anti-PD-L1 efficacy in preclinical models of," 2018, Accessed: Apr. 03, 2020. [Online]. Available: https://cancerres.aacrjournals.org/content/78/13_Supplement/1017.short.

[50] X. Chen, S. Ciren, H. Zhang, … L. D.-W. J. of, and undefined 2009, "Effect of 5-FU on modulation

of disarrangement of immune-associated cytokines in experimental acute pancreatitis," *ncbi.nlm.nih.gov*, Accessed: Apr. 03, 2020. [Online]. Available: https://www.ncbi.nlm.nih.gov/pmc/articles/PMC2675097/.

[51] S. Marino, I. B. Hogue, C. J. Ray, and D. E. Kirschner, "A methodology for performing global uncertainty and sensitivity analysis in systems biology," *Journal of Theoretical Biology*, vol. 254, no. 1. Academic Press, pp. 178–196, Sep. 07, 2008, doi: 10.1016/j.jtbi.2008.04.011.

[52] F. Pianosi, F. Sarrazin, T. W.-E. M. & Software, and undefined 2015, "A Matlab toolbox for global sensitivity analysis," *Elsevier*, Accessed: Apr. 03, 2020. [Online]. Available: https://www.sciencedirect.com/science/article/pii/S1364815215001188.

[53] S. Shafiekhani, S. Rahbar, F. Akbarian, and A. H. Jafari, "Fuzzy Stochastic Petri Net with Uncertain Kinetic Parameters for Modeling Tumor-Immune System," 2019, doi: 10.1109/ICBME.2018.8703573.

Figures

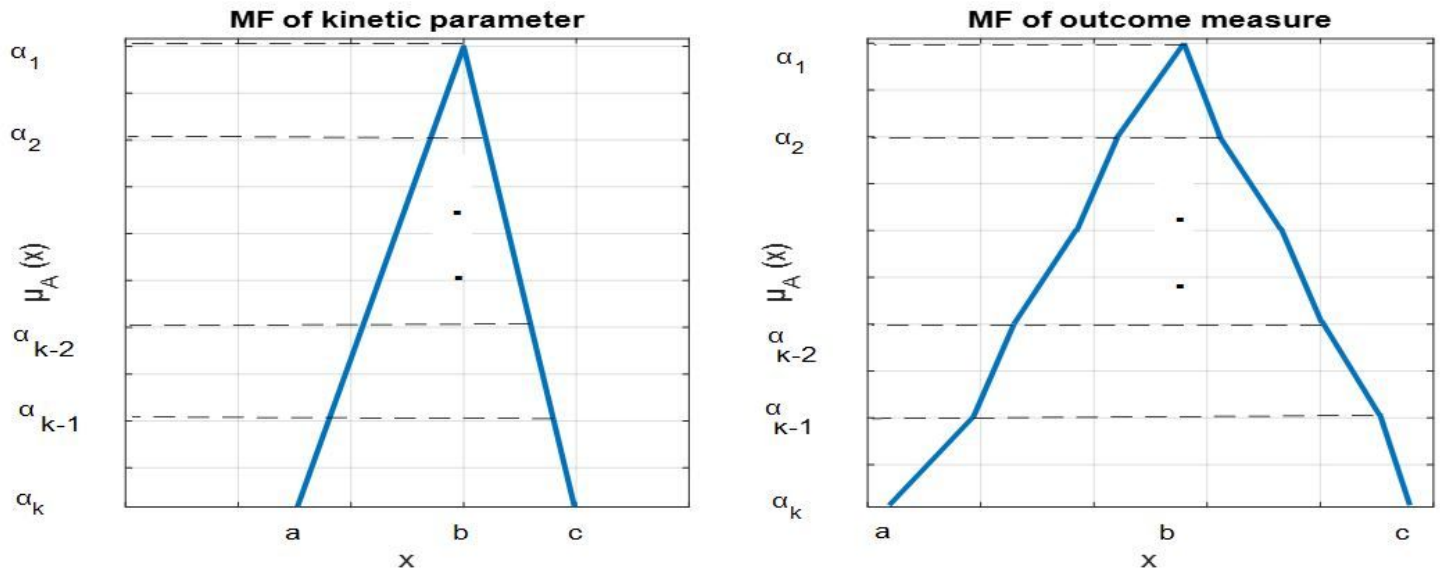

Figure 1

(Left) Decomposition of a fuzzy uncertain kinetic parameter to its α-cuts and (right) composition of a set of α-cuts to create a membership function for fuzzy uncertain outcome measure.

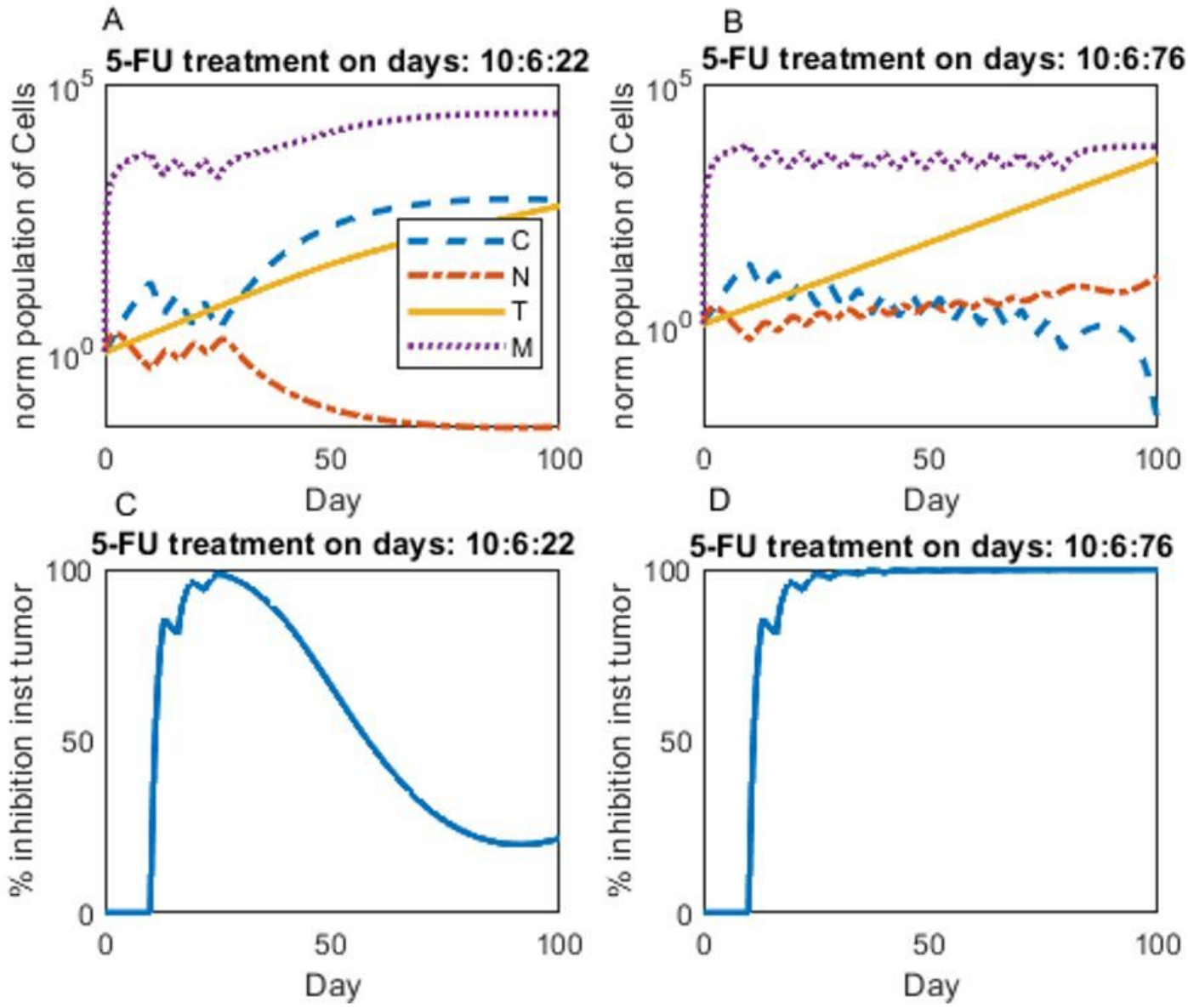

Figure 2

Dynamics of tumor cells, NK, CTL, and MDSC in response to different timing of 5-FU treatment over time along with efficacy assessment of 5-FU treatment with regarding crisp values for kinetic parameters of model. (A) The dynamics of cancer cells, NK cells, CTLs and MDSCs (normalized to initial population) affected by 5-FU treatment on days 10, 16 and 22 after tumor injection on day 0 and (B) by 5-FU treatment on days 10, 16, 22, 28, 34, 40, 46, 52, 58, 64, 70 and 76 after tumor injection on day 0. (C) The instantaneous inhibition percentage of tumor cells affected by 5-FU on days 10:6:22 and (D) by 5-FU treatment on days 10:6:76.

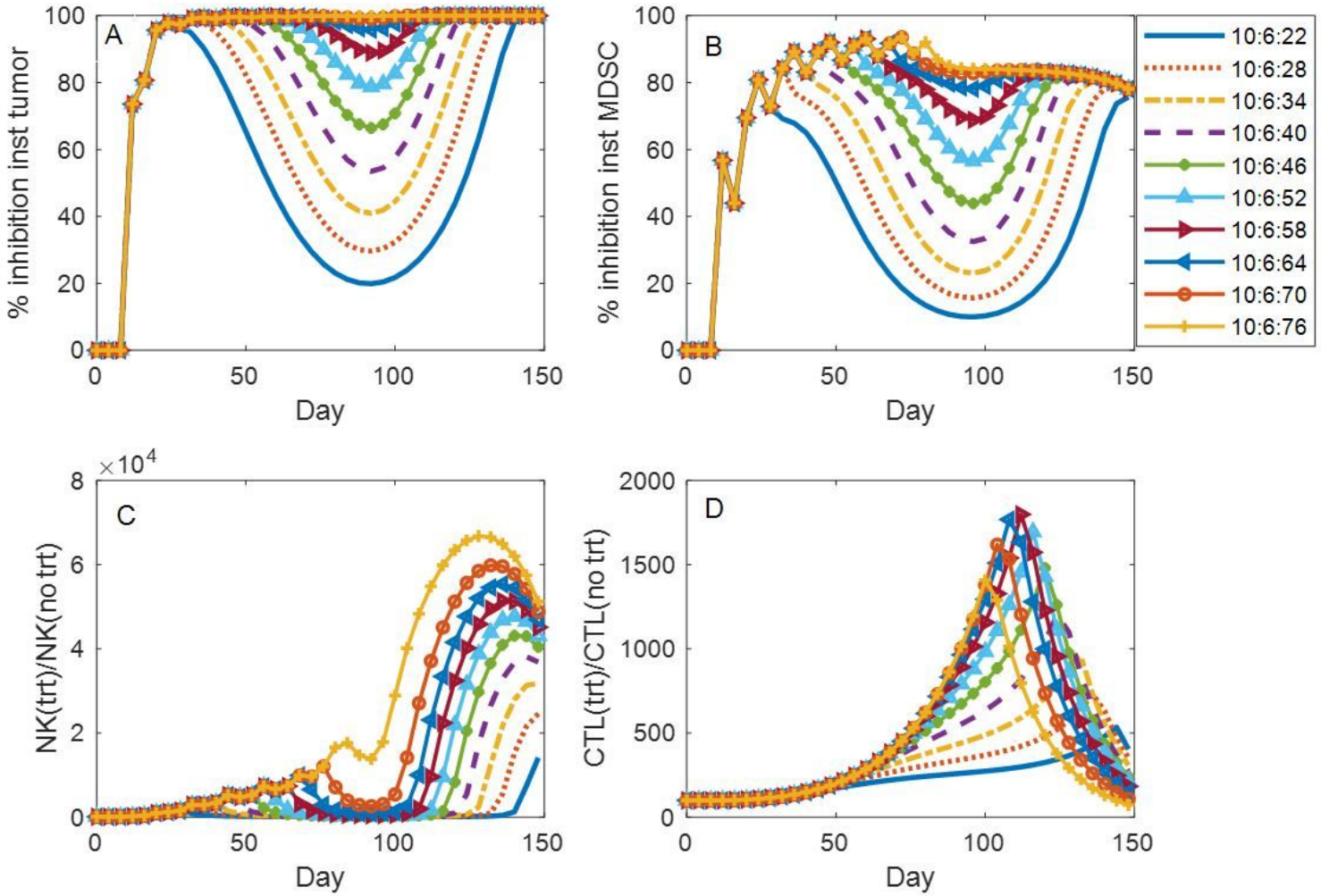

Figure 3

Prediction of the effect of different timing of 5-FU treatment on TISTIS cells population. The treatment efficacy for different timing of 5-FU was plotted as percentage of instantaneous tumor growth inhibition (A) and percentage of instantaneous MDSC expansion inhibition (B). The ratio of population of NK cells (C) and CTLs (D) in different timing of 5-FU treatment to their population in control case (no treatment).

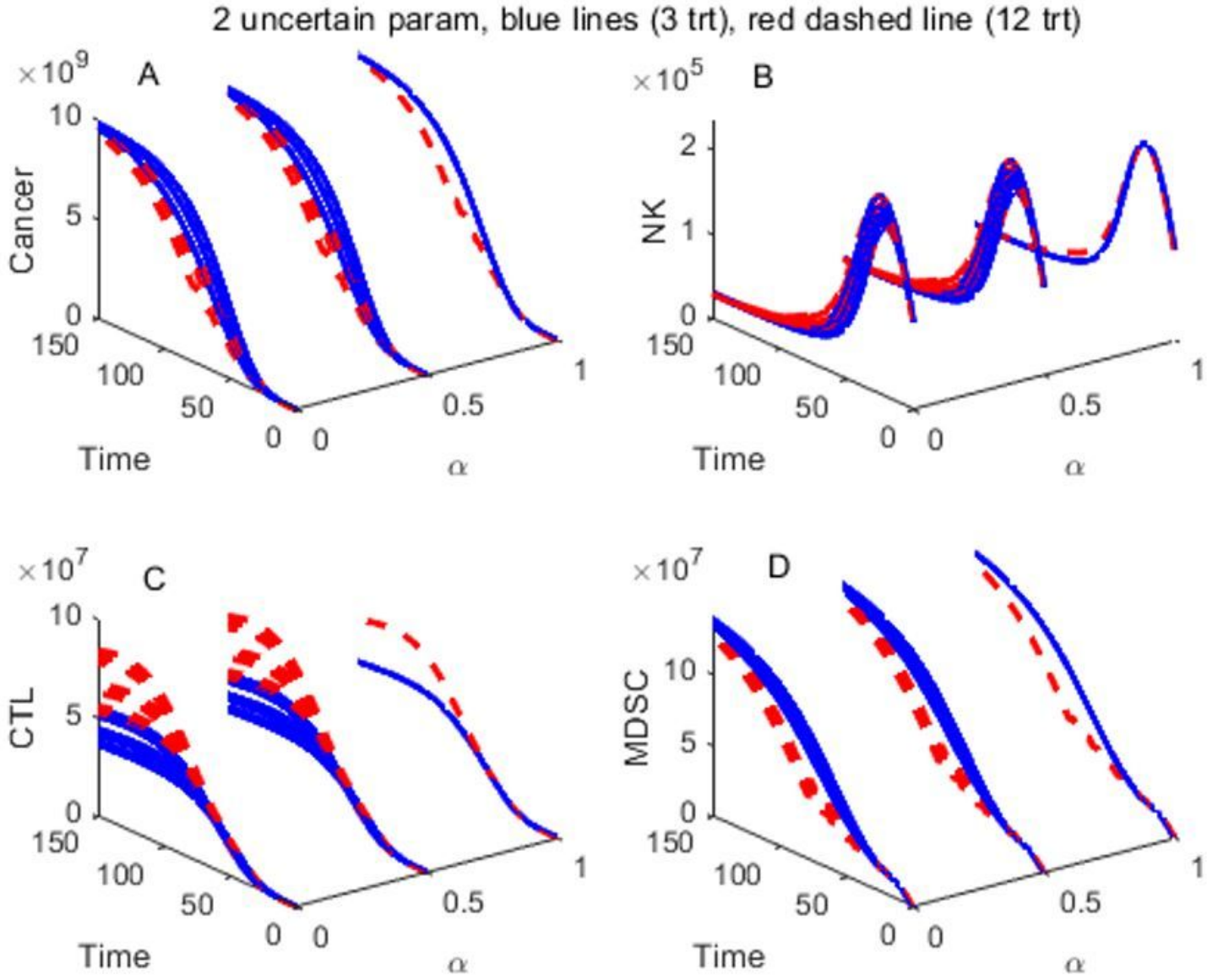

Figure 4

A three-dimensional simulation plot of cancer cells (A), NK cells (B), CTLs(C) and MDSCs (D) for two different timing of 5-FU treatment (same as those given in Figure 2) in fuzzy setting of kinetic parameters. The two fuzzy uncertain numbers are given as follow: a= (0.9,1,1.1)×1.45×10^(-1) and f= (0.9,1,1.1)× 4.12×10^(-2).

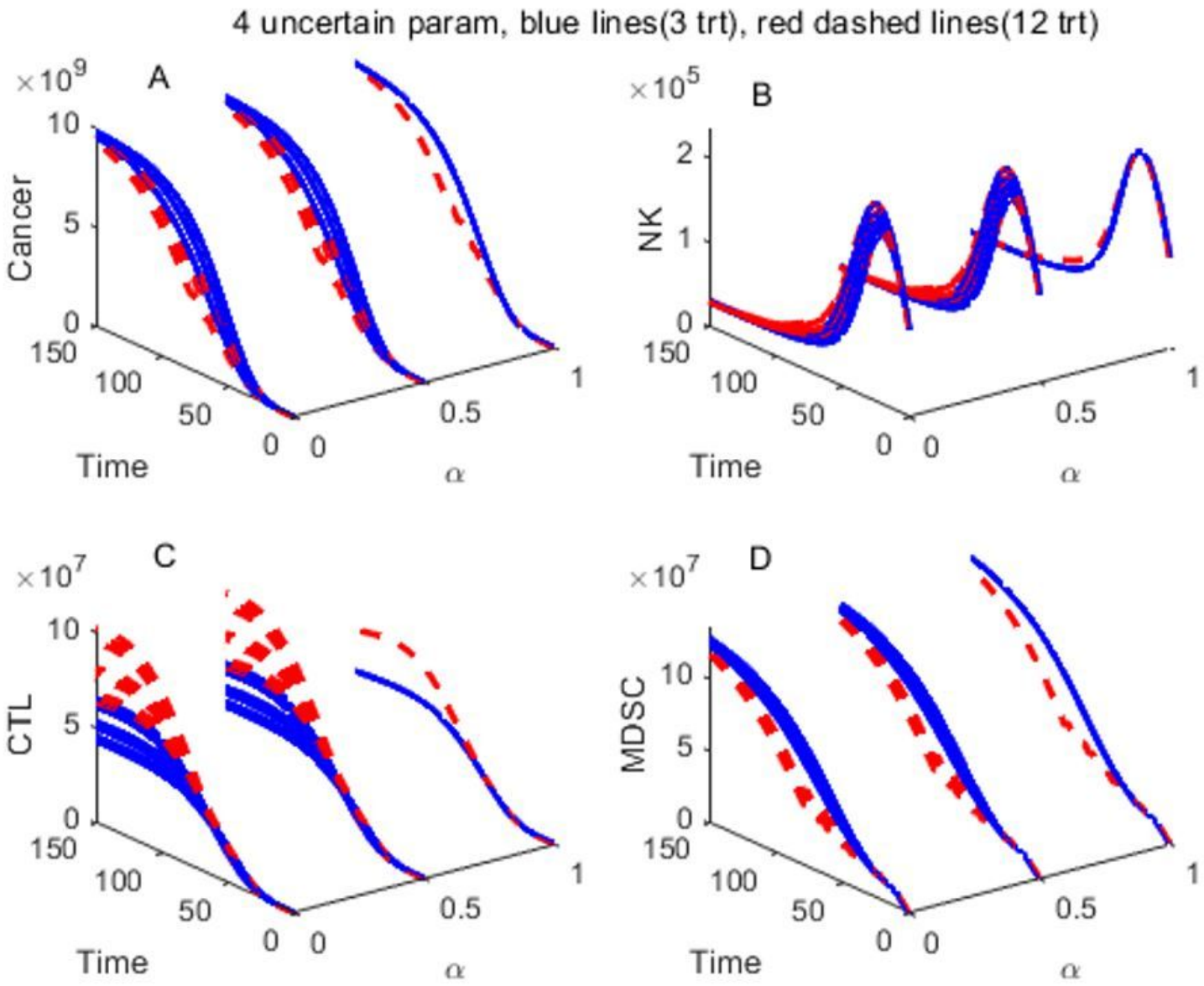

Figure 5

A three-dimensional simulation plot of cancer cells(A), NK cells (B), MDSCs (C) and CTLs (D) for two different timing of 5-FU treatment (same as those given in Figure 2) in fuzzy setting of kinetic parameters. The four fuzzy uncertain numbers are given as follow: a= (0.9,1,1.1)×1.45×10^(-1), f= (0.9,1,1.1)× 4.12×10^(-2),m= (0.9,1,1.1)×2×10^(-2) and α= (09,1,1.1)×7×10^6.

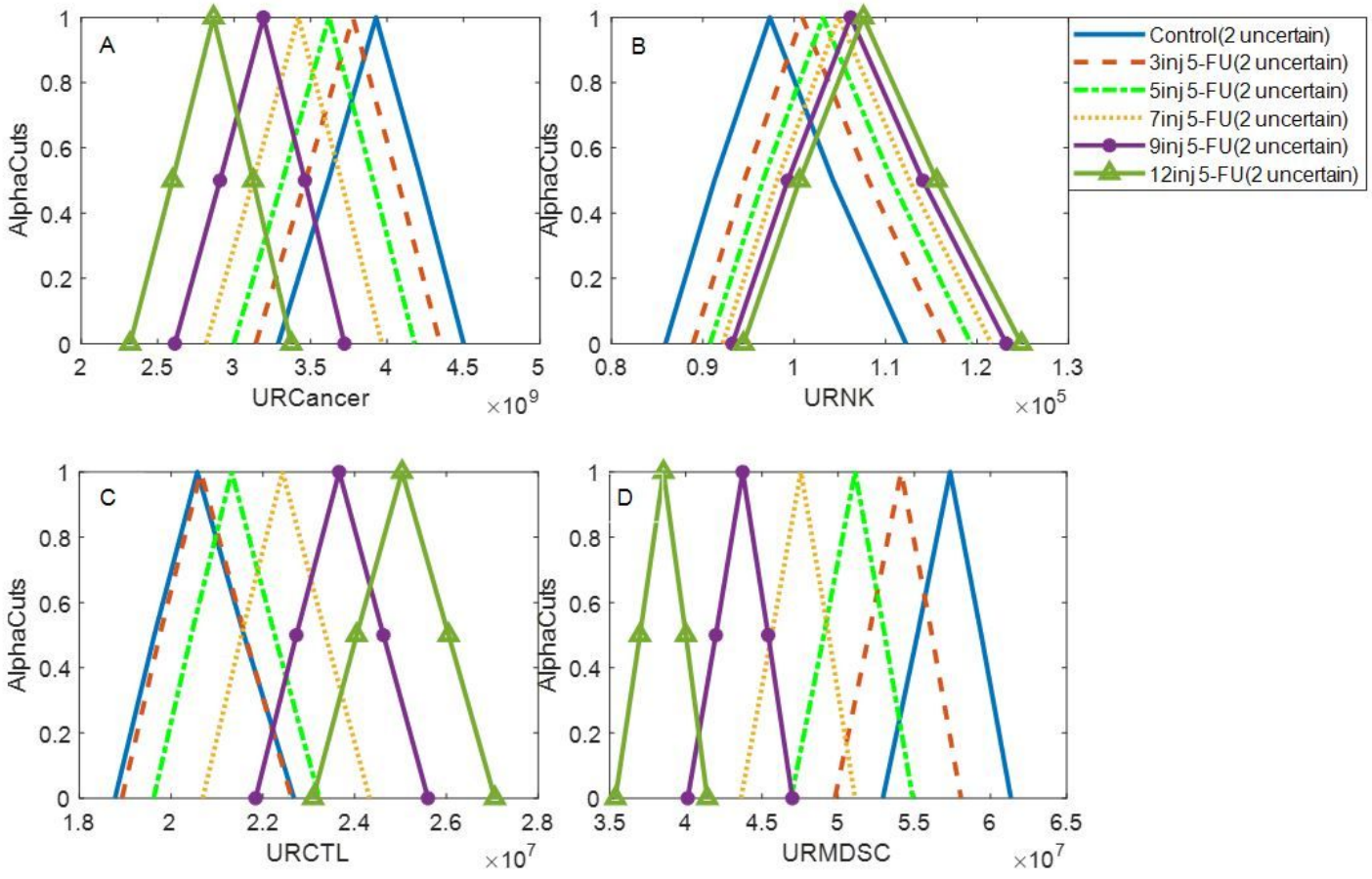

Figure 6

The membership function of average of dynamics of cancer cells (A), NK cells (B), CTLs(C) and MDSCs (D) in the time interval from day 10 to day 100 (after first 5-FU injection) for different timing of 5-FU injection (10:6:22, 10:6:34, 10:6:46, 10:6:58, 10:6:76) in fuzzy setting of kinetic parameters. The two fuzzy uncertain numbers are given as follow: a= (0.9,1,1.1)×1.45×10^(-1) and f= (0.9,1,1.1)× 4.12×10^(-2).

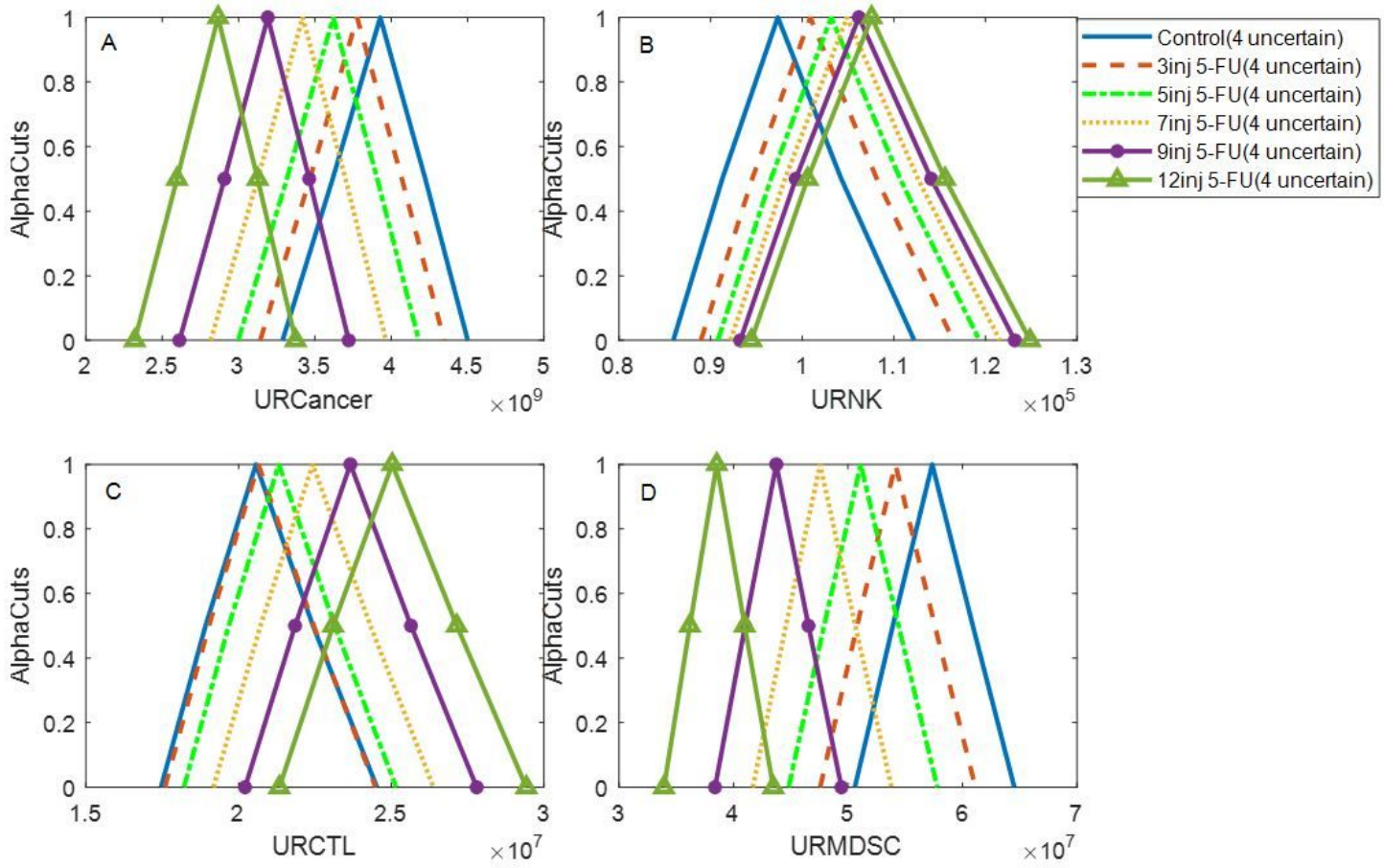

Figure 7

The membership function of average of dynamics of cancer cells (A), NK cells (B), CTLs(C) and MDSCs (D) in the time interval from day 10 to day 100 (after first 5-FU injection) for different timing of 5-FU injection (10:6:22, 10:6:34, 10:6:46, 10:6:58, 10:6:76) in fuzzy setting of kinetic parameters. The four fuzzy uncertain numbers are given as follow: a= (0.9,1,1.1)×1.45×10^(-1), f= (0.9,1,1.1)× 4.12×10^(-2),m= (0.9,1,1.1)×2×10^(-2) and α= (09,1,1.1)×7×10^6.

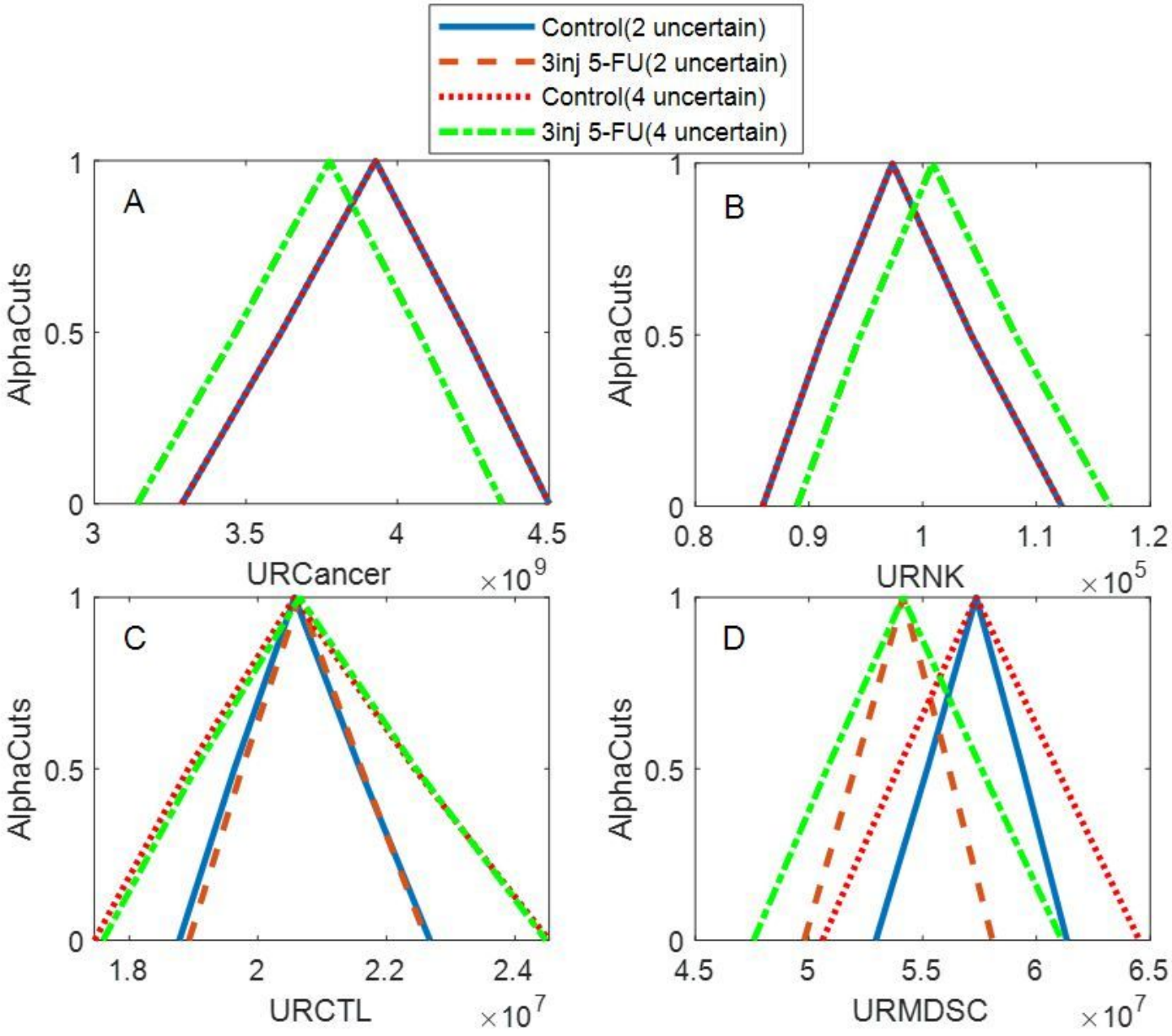

Figure 8

The membership function of average of dynamics of TIS' cells in the time interval from day 10 to day 100 (after first 5-FU injection) in control group (no treatment) and 5-FU treatment group (on day 10:6:22 after tumor inoculation) and in two different fuzzy settings (two or four fuzzy uncertain kinetic parameters). (A) shows the membership function of averaged dynamics of cancer cells in control compared with 5–FU treatment group and with regarding two fuzzy parameters (same as those given in figure 4) or four fuzzy parameters (same as those given in figure 5). (A), (B), (C) and (D) depict the membership function of averaged dynamics of cancer cells, NK cells, CTLs and MDSCs, respectively. The blue solid line depicts the membership function of fuzzy uncertain outcome measures (cancer cells, NK cells, CTLs and MDSCs) in control group (no treatment) with regarding two fuzzy uncertain kinetic parameters (same as figure 4), the brown dashed lines shows for 5-FU treatment (three times) and two fuzzy parameters, the red dotted

line shows for control group and four fuzzy uncertain parameters, and green dash-dotted line depicts for 5-FU treatment (three times) and four uncertain parameters.

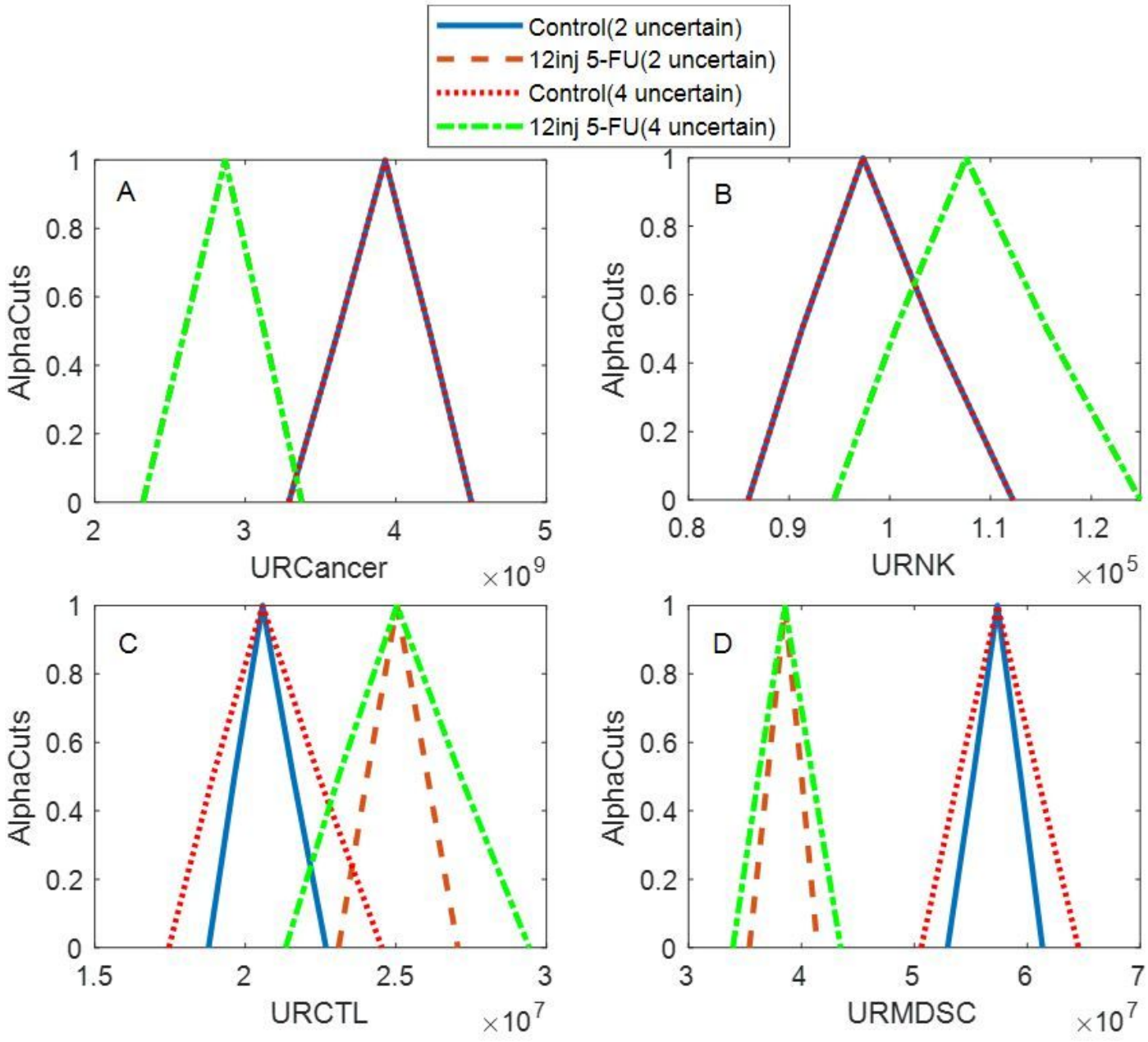

Figure 9

The membership function of average of dynamics of TIS' cells in the time interval from day 10 to day 100 (after first 5-FU injection) in control group (no treatment) and 5-FU treatment group (on day 10:6:76 after tumor inoculation) and in two different fuzzy settings (two or four fuzzy uncertain kinetic parameters). (A) shows the membership function of averaged dynamics of cancer cells in control compared with 5–FU treatment group and with regarding two fuzzy parameters (same as those given in figure 4) or four fuzzy parameters (same as those given in figure 5). (A), (B), (C) and (D) depict the membership function of averaged dynamics of cancer cells, NK cells, CTLs and MDSCs, respectively. The blue solid line depicts the membership function of fuzzy uncertain outcome measures (cancer cells, NK cells, CTLs and MDSCs)

in control group (no treatment) with regarding two fuzzy uncertain kinetic parameters (same as figure 4), the brown dashed lines shows for 5-FU treatment (ten times) and two fuzzy parameters, the red dotted line shows for control group and four fuzzy uncertain parameters, and green dash-dotted line depicts for 5-FU treatment (ten times) and four uncertain parameters.

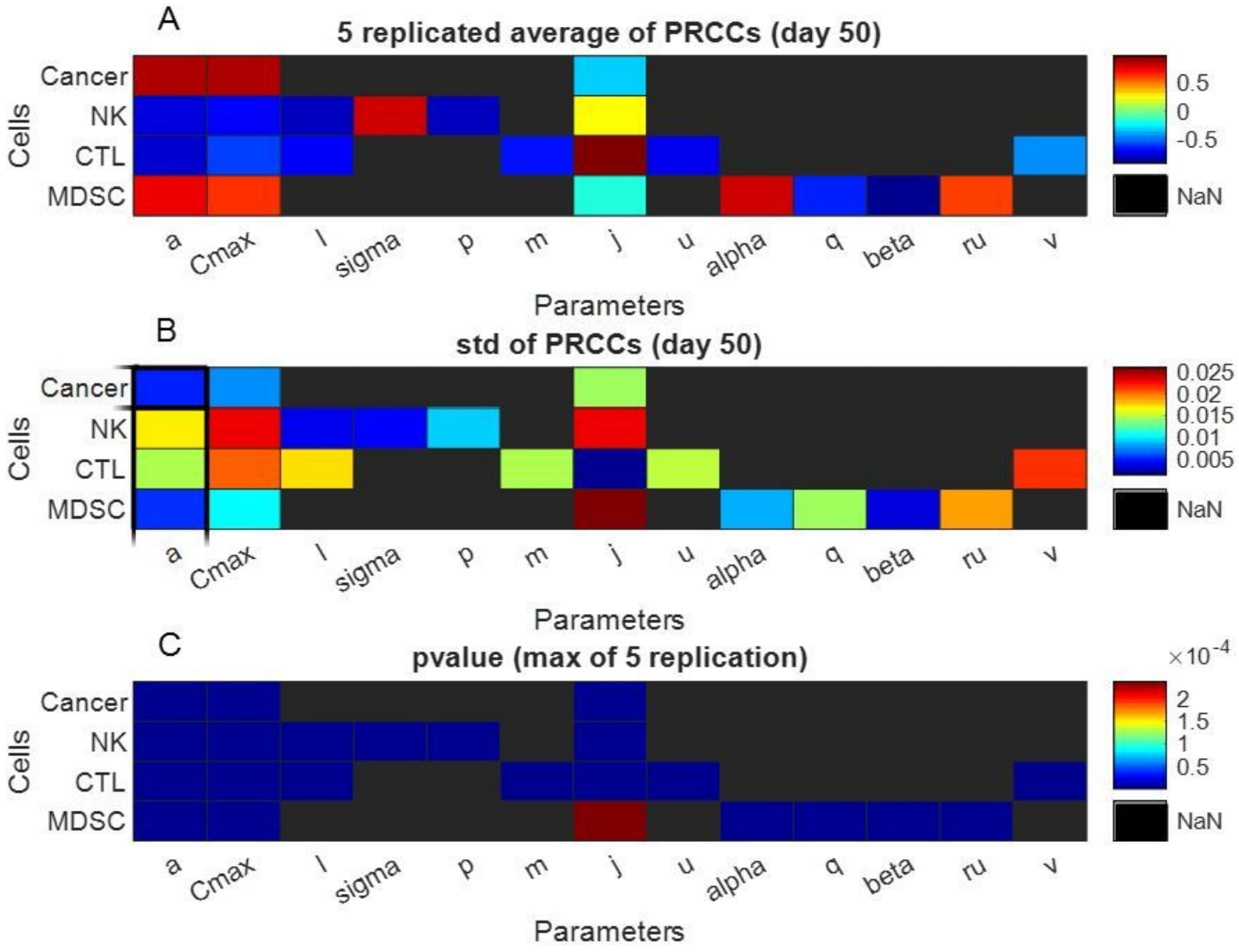

Figure 10

Statistically significant PRCC values (p-value<0.05) for tumor cells, NK cells, CTLs and MDSCs at day 50 after tumor injection. The first and second panels show the mean and standard deviation of PRCC values for five replications of PRCC analysis and the third panel depicts the maximum of their corresponding p-values. Black pixels (NaN) show ‘not a number’ and represent no significant correlation between outcome measures (population of cells, elements in vertical axis) and kinetic parameters of model (elements in horizontal axis).

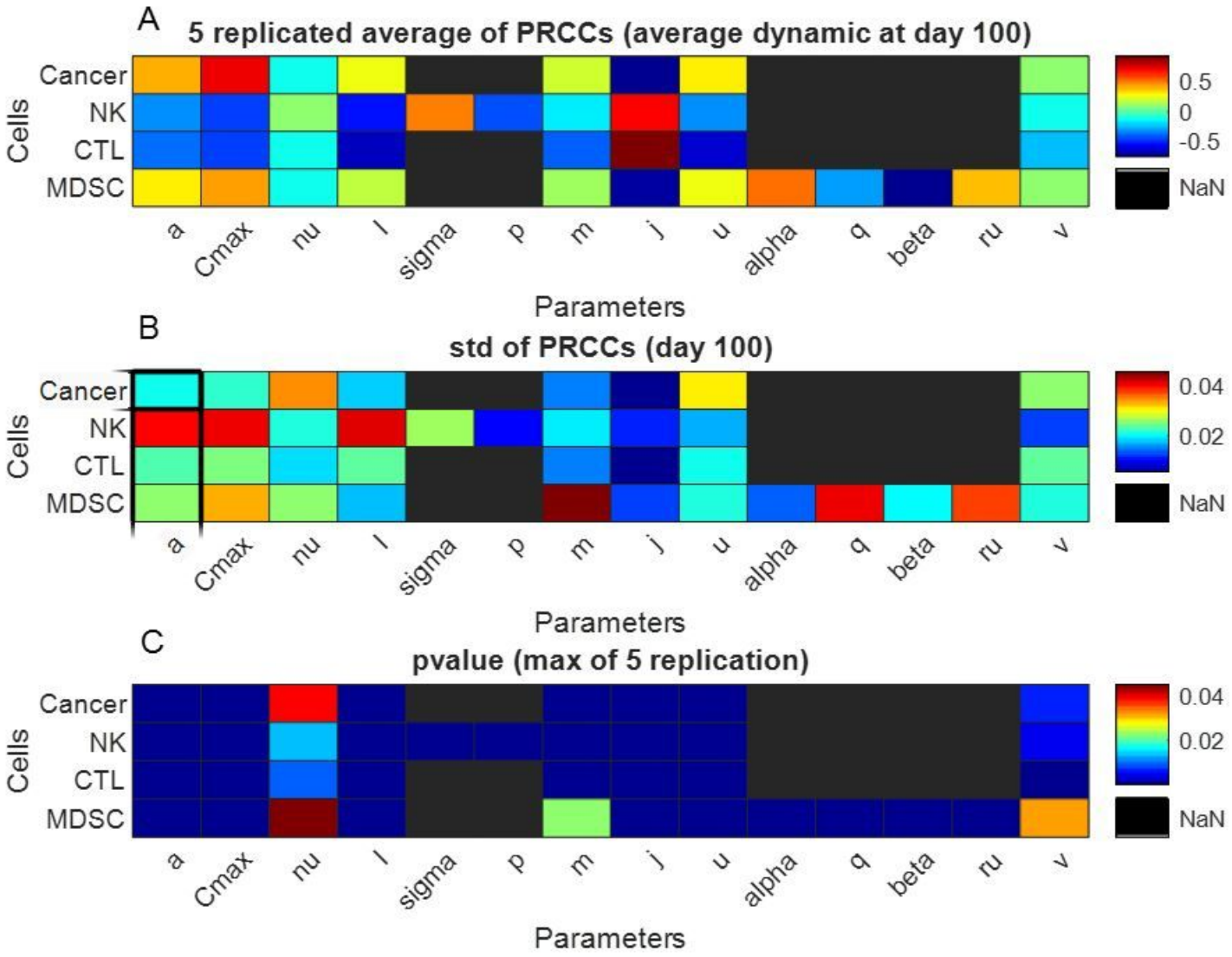

Figure 11

Statistically significant PRCC values (p-value<0.05) for tumor cells, NK cells, CTLs and MDSCs at day 100 after tumor injection. The first and second panels show the mean and standard deviation of PRCC values for five replications (or five replicates) of PRCC analysis and the third panel depicts the maximum of PRCC corresponding p-values. Black pixels (NaN) shows 'not a number' and represents no significant correlation between outcome measures (population of cells, its element in vertical axis) and kinetic parameters of model (element in horizontal axis).

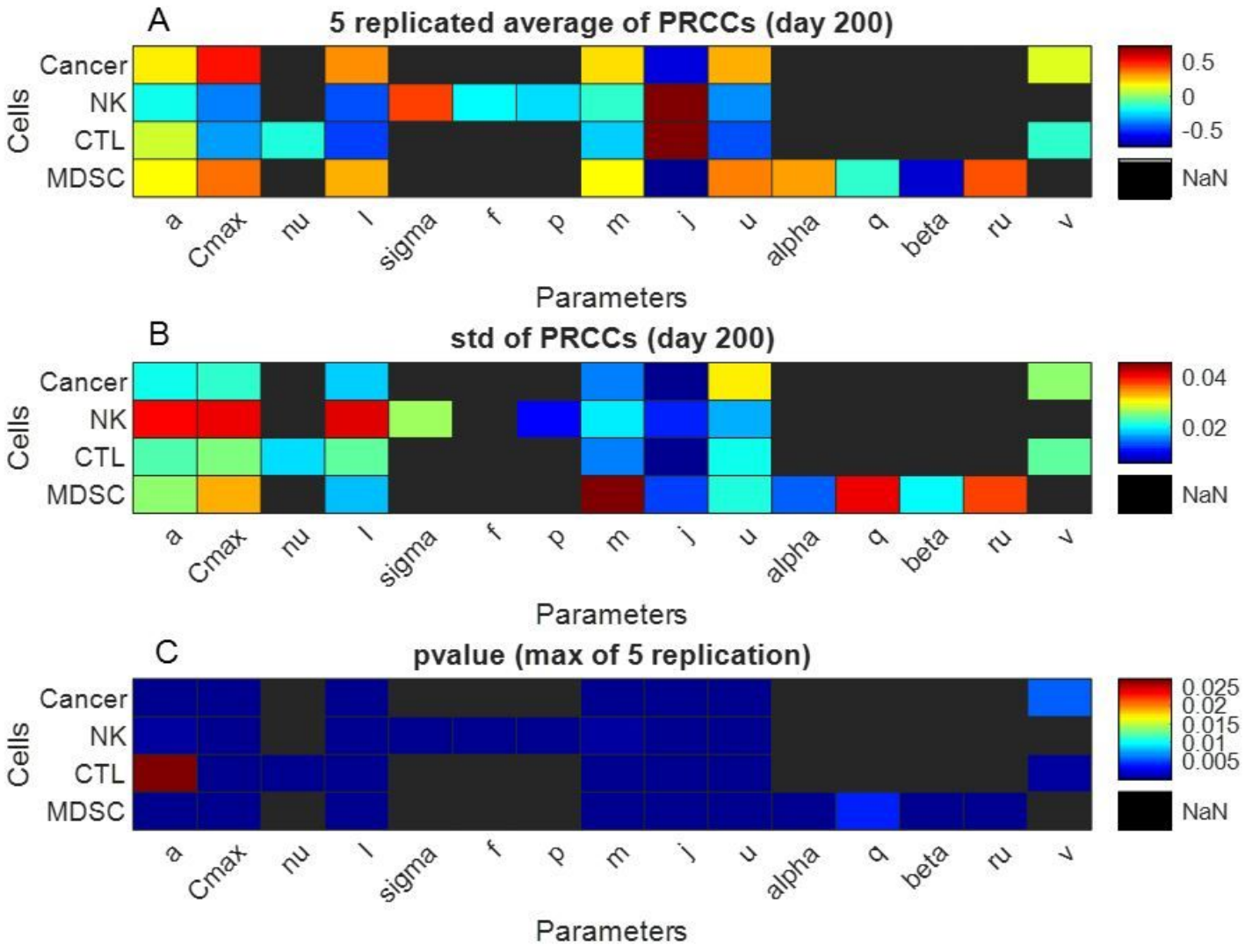

Figure 12

Statistically significant PRCC values (p-value<0.05) for tumor cells, NK cells, CTLs and MDSCs at day 200 after tumor injection. The first and second panels show the mean and standard deviation of PRCC values for five replication or five replicates of PRCC analysis and the third panel depicts the maximum of PRCC corresponding p-values. Black pixels (NaN) shows ‘not a number’ and represents no significant correlation between outcome measures (population of cells, elements in vertical axis) and kinetic parameters of model (element in horizontal axis).

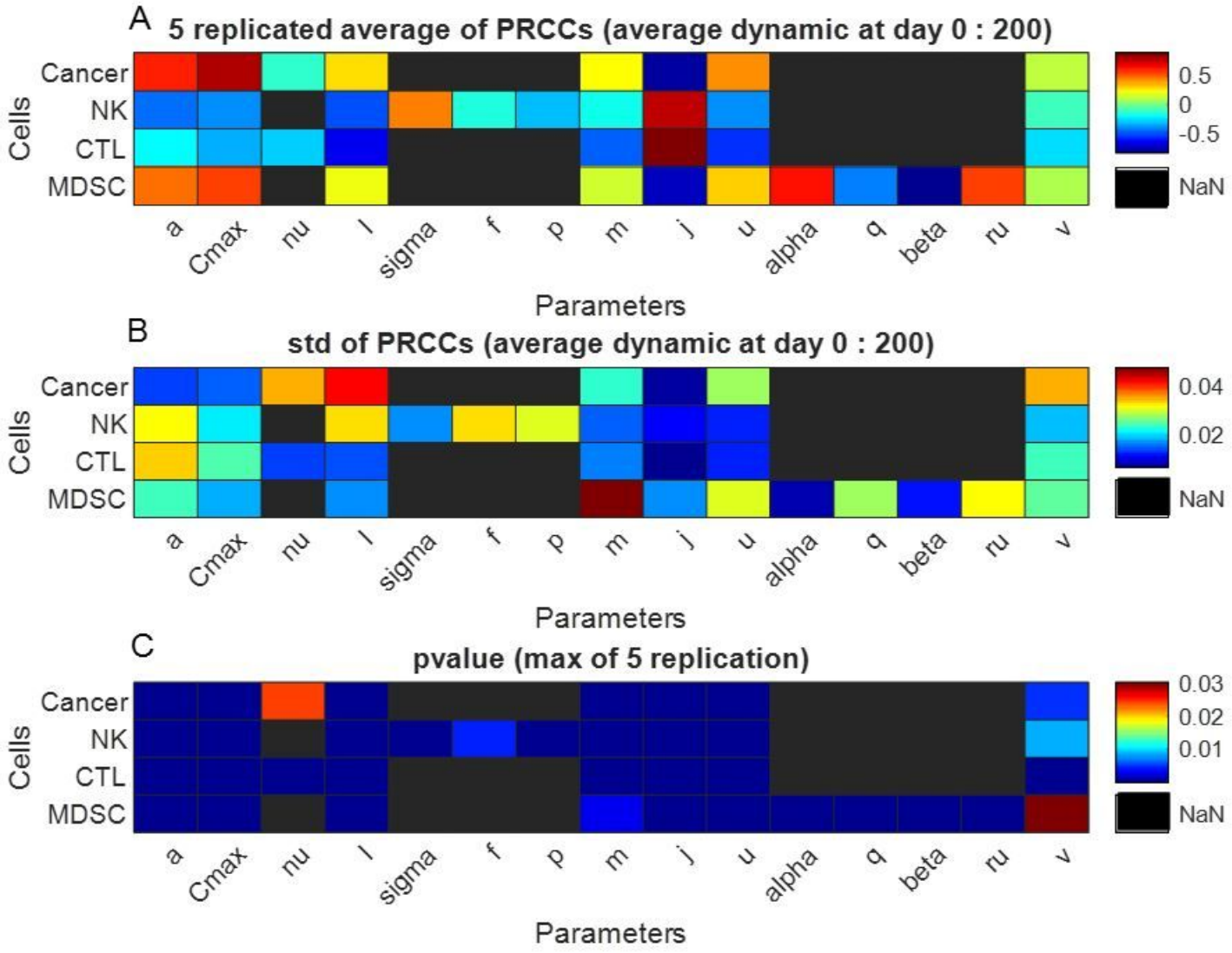

Figure 13

Statistically significant PRCC values (p-value<0.05) for an average of dynamics of tumor cells, NK cells, CTLs and MDSCs in the time interval from day 0 to day 200 after tumor injection. The first and second panels show the mean and standard deviation of PRCC values for five replications of PRCC analysis and the third panel depicts the maximum of PRCC corresponding p-values. Black pixels (NaN) shows ‘not a number’ and represents no significant correlation between outcome measures (population of cells, elements in vertical axis) and kinetic parameters of model (element in horizontal axis).

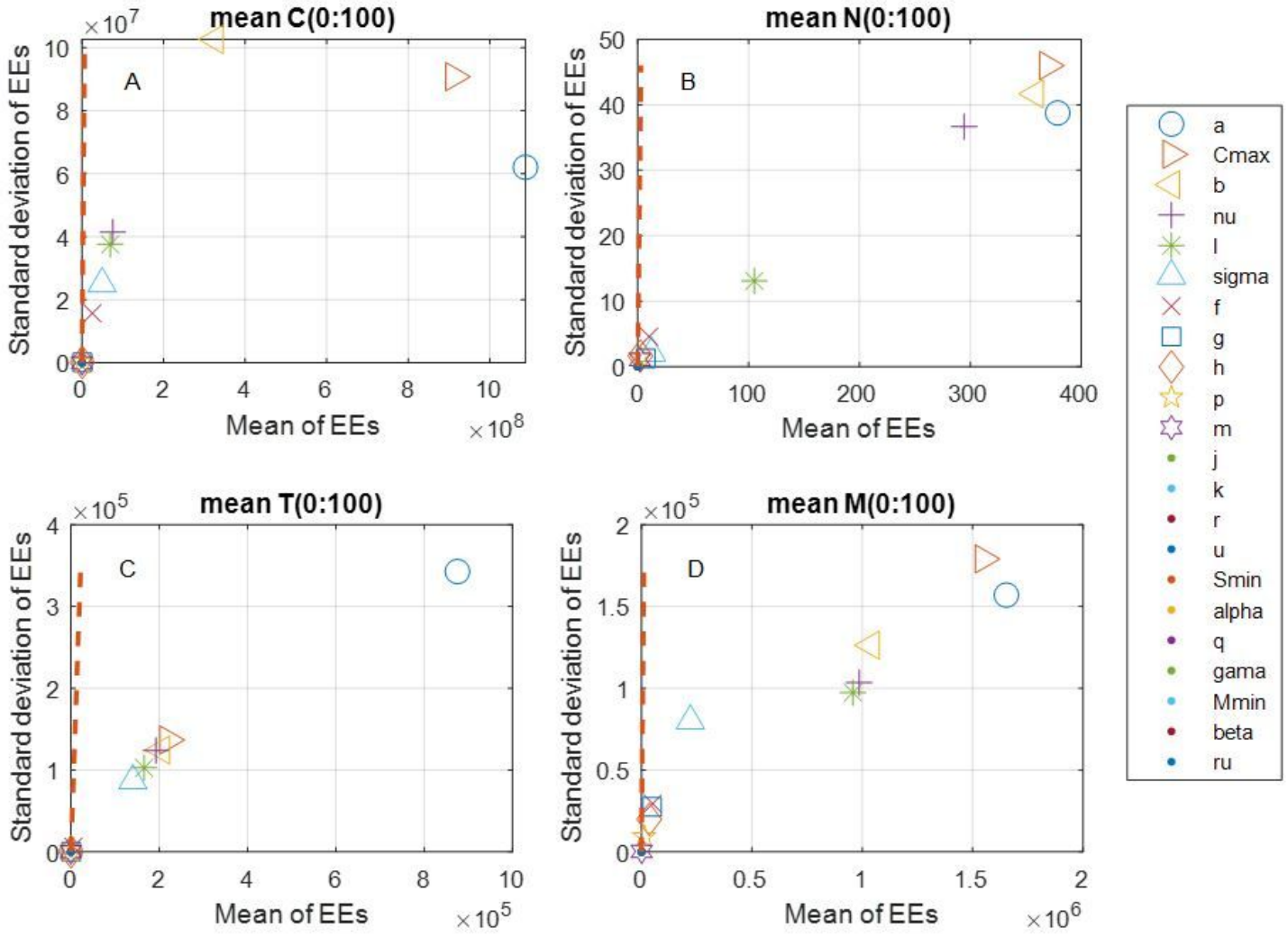

Figure 14

The absolute mean value and standard deviation of Morris GSA (elementary effects analysis). Figures present the relative importance of kinetic parameters of TIS model, considering the mean population of tumor cells (A), mean population of NK cells (B), mean population of CTLs (C) and mean population of MDSCs (D) from day 0 to day 100 as read-out. Each kinetic parameter is specified by two Morris indices, σ (vertical axis) and μ*(horizontal axis), which describe the interaction or nonlinear effects and the significance of the effects, respectively.

Supplementary Files

This is a list of supplementary files associated with this preprint. Click to download.

- Highlightreview.docx
- Tables.docx